

UNCLASSIFIED

AD 263 597

*Reproduced
by the*

**ARMED SERVICES TECHNICAL INFORMATION AGENCY
ARLINGTON HALL STATION
ARLINGTON 12, VIRGINIA**



UNCLASSIFIED

NOTICE: When government or other drawings, specifications or other data are used for any purpose other than in connection with a definitely related government procurement operation, the U. S. Government thereby incurs no responsibility, nor any obligation whatsoever; and the fact that the Government may have formulated, furnished, or in any way supplied the said drawings, specifications, or other data is not to be regarded by implication or otherwise as in any manner licensing the holder or any other person or corporation, or conveying any rights or permission to manufacture, use or sell any patented invention that may in any way be related thereto.

263597

CATALOGED IN ASTIA
AS AD NO.

U. S. A R M Y
TRANSPORTATION RESEARCH COMMAND
FORT EUSTIS, VIRGINIA

TCREC TECHNICAL REPORT 61-93

THE INFLUENCE OF TWO-DIMENSIONAL STREAM SHEAR
ON AIRFOIL MAXIMUM LIFT

Project 9R38-01-000, Task 902

Contract DA 44-177-TC-439

August 1961

prepared by :

CORNELL AERONAUTICAL LABORATORY, INC.,
BUFFALO, NEW YORK

N8X-45
~~XXXX~~



ASTIA
RECEIVED
OCT 4 1961
JIPOR A

DISCLAIMER NOTICE

When Government drawings, specifications, or other data are used for any purpose other than in connection with a definitely related Government procurement operation, the United States Government thereby incurs no responsibility nor any obligation whatsoever; and the fact that the Government may have formulated, furnished, or in any way supplied the said drawings, specifications, or other data is not to be regarded by implication or otherwise as in any manner licensing the holder or any other person or corporation, or conveying any rights or permission, to manufacture, use, or sell any patented invention that may in any way be related thereto.

ASTIA AVAILABILITY NOTICE

Qualified requestors may obtain copies of this report from

Armed Services Technical Information Agency
Arlington Hall Station
Arlington 12, Virginia

This report has been released to the Office of Technical Services, U. S. Department of Commerce, Washington 25, D. C., for sale to the general public.

This information contained herein will not be used for advertising purposes.

The findings and recommendations contained in this report are those of the contractor and do not necessarily reflect the views of the Chief of Transportation or the Department of the Army.



CORNELL AERONAUTICAL LABORATORY, INC.
OF CORNELL UNIVERSITY
BUFFALO 21, NEW YORK

REPORT NO. A1-1190-A-7

THE INFLUENCE OF TWO-DIMENSIONAL STREAM SHEAR
ON AIRFOIL MAXIMUM LIFT

AUGUST 1961

PROJECT 9R-38-01-000, TASK 902

CONTRACT DA 44-177-TC-439

U.S. ARMY TRANSPORTATION RESEARCH COMMAND
TRANSPORTATION CORPS
FORT EUSTIS, VIRGINIA

BY: R. J. Vidal
R. J. Vidal

APPROVED BY: A. Hertzberg
A. Hertzberg, Head
Aerodynamic Research Dept.

James T. Curtin
J. T. Curtin

J. H. Hilton
J. H. Hilton

ASTIA
OCT 4 1961
TIPDR A

HEADQUARTERS
U. S. ARMY TRANSPORTATION RESEARCH COMMAND
Fort Eustis, Virginia

FOREWORD

This report, based upon a paper presented at the National IAS/ARS Joint Meeting in June 1961, presents the results of research performed by the authors at Cornell Aeronautical Laboratory, Inc., Buffalo, New York, under Army Contract DA 44-177-TC-439, Project Number 9-38-01-000, ST902. The U. S. Army Transportation Research Command, Fort Eustis, Virginia, is the monitoring agency. This work represents a part of a research program, still in progress, which is devoted to general research on the aerodynamics of low-speed flight, as well as the investigations of several specific problems associated with STOL/VTOL flight. This report is one of a series to be published covering the entire program of research.

The report has been reviewed by this Command and is considered to be technically sound. The report is published for the exchange of information and the stimulation of ideas.

FOR THE COMMANDER:

APPROVED BY:


JAMES G. MC HUGH
USATRECOM Project Engineer

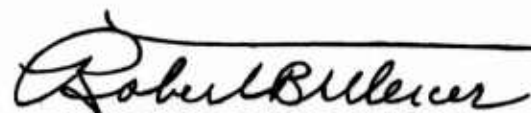

ROBERT B. MERCER
Captain, TC
Asst Adjutant



TABLE OF CONTENTS

List of Symbols	ii
Introduction	1
Theories for Airfoils in Shear Flow	3
Uniform Shear	3
Nonuniform Shear	6
Experiments on Airfoil Stall in Shear Flow	12
Apparatus	12
Force Data	14
Oil Film Studies	17
Thickness-Shear Interaction	20
Influence of Stream Shear on Boundary Layer Separation	22
Pressure Distribution	22
The Laminar Boundary Layer with External Shear	26
Concluding Remarks	35
Appendix - The Thickness-Shear Interaction in Nonuniform Shear Flow	37
References	43
Distribution	58

LIST OF SYMBOLS

U	velocity
U_0	undisturbed stream velocity at the airfoil position
x, y	coordinates parallel and normal to the stream
c	reference chord length
k_2	local stream shear $\frac{\tau}{U_0} \frac{dU_0}{dy}$
L	lift
M	pitching moment about the airfoil midchord station
α	angle of attack
ρ	density
τ	airfoil thickness-chord ratio
h	maximum height of the airfoil camber line
H	transformation length
g	parameter defining nonuniform shear
U_∞	reference velocity at the stream plane of symmetry
ψ	stream function
r	half height of the two-dimensional slipstream
α_n, β_n	see Eq. (10)
σ	$1 + \frac{1}{2} g \ln g$
ϕ	see Eq. (11)
u, v	velocities in the boundary layer parallel to and normal to the surface
p	pressure
ν	kinematic viscosity
δ	boundary-layer thickness

δ^*	displacement thickness
θ	momentum thickness
ϵ	see Fig. 14
η	y/δ
U_δ	velocity at the outer edge of the boundary layer
Λ	$\frac{\delta^2}{\nu} \frac{\partial U}{\partial x}$
λ	$\frac{\rho \delta^2 U_\delta}{2 H^2 U_\delta}$
ξ	$\frac{\rho \delta U_\delta (\epsilon - \delta^*)}{2 H^2 U_\delta}$

INTRODUCTION

The Cornell Aeronautical Laboratory is conducting a program of theoretical and experimental research on low-speed aerodynamics as applied to STOL and VTOL aircraft. The objective of this program is to re-examine certain aspects of classical aerodynamic information, in the light of low-speed flight requirements, with the aim of seeking aerodynamic processes which might be exploited to enhance low-speed performance.

One aspect of propeller-driven aircraft which has recently received increasing attention is the existence of strong gradients of longitudinal velocity, or shear, in the propeller slipstream. This slipstream shear interacts with a wing surface and can alter the wing characteristics. In theoretical treatments of a wing interacting with a propeller slipstream, the first important simplification is the replacement of the slipstream with an ideal uniform jet, free of all velocity gradients. The application of these theories requires that one equate the actual slipstream to an effective uniform jet. One method employed is to assume the uniform jet has a momentum flux equal to the average in the propeller slipstream. These and similar procedures are well founded on momentum considerations; however, the implicit assumption is that the flow nonuniformity, the shear, does not influence the wing characteristics.

In the interests of clarifying this aspect of the wing-propeller slipstream problem, a theoretical and experimental investigation was conducted to quantitatively determine the effects of stream shear on airfoil characteristics. In the theoretical study, the problem was reduced to its most elementary form in order to isolate the inviscid effects of shear. This

investigation was then followed by systematic experimental research to check and to extend these results to the more practical situation of a wing interacting with an actual propeller slipstream.

This experimental research provided the desired verification and extension of the theoretical results. In addition, the results showed that the airfoil maximum lift varied markedly when the airfoil was positioned at various locations in the shear stream. The change in airfoil maximum lift with stream shear was explored in detail in a subsequent experimental study. These latter experiments showed that, in one instance, by repositioning the airfoil in the shear stream through a distance comparable to the airfoil thickness, the airfoil maximum lift was doubled. Further inviscid and viscid theoretical studies were made to isolate and explain this destalling phenomenon.

The purpose of this paper is to present both experimental data on airfoil maximum lift in a two-dimensional shear stream and theoretical studies devoted to explaining these results. In this connection, the available inviscid theories for airfoils in uniform and nonuniform shear flows will be briefly reviewed to illustrate the inviscid effects of stream shear on airfoil characteristics. The experimental data showing the destalling phenomena will then be discussed, and the results of the theoretical studies will be presented to illustrate the effects of shear on airfoil stall.

THEORIES FOR AIRFOILS IN SHEAR FLOW

The problem of the influence of stream nonuniformities or stream shear on airfoil characteristics is, of course, not new. This problem has existed virtually since the introduction of the airplane, and sporadic attention has been given to the problem since then. Concerted attention to the problem has not been warranted until now, since the emphasis in propeller-driven airplanes has been on propellers which perturb the flow slightly, and the slipstream shear was accordingly small. The current interest in diminishing aircraft take-off and landing distances has had two effects; first, it has made take-off and landing considerations of paramount importance, and second, it has emphasized propellers producing large flow perturbations. This latter fact implies that the slipstream will possess large shear, and consequently requires that the influence of shear on airfoil characteristics be re-examined.

Uniform Shear

The effect of uniform stream shear was first treated by von Sanden¹ in 1912. In this work, consideration was restricted to a wedge profile in a stream with a linear velocity gradient, i. e. uniform shear, and a numerical solution was obtained. This same problem was taken up again by Tsien² in 1943, in connection with the influence of ground level gradients in wind velocity on airfoil characteristics. In his investigation, Tsien considered a symmetrical two-dimensional Joukowski airfoil in an inviscid stream of indefinite extent with uniform shear, and obtained an exact solution for the airfoil forces. The interest in deflected slipstream configurations with highly flapped wings led to an extension of Tsien's theory by Sowyrda³ in 1958 to the case of a cambered airfoil in a stream with uniform shear.

Again, an exact inviscid solution was obtained, valid for any thickness, camber, and angle of attack. The model considered both by Tsien and by Sowyrda is illustrated in Fig. 1. One important feature of this model is that the entire system, both airfoil and stream, is two-dimensional and moreover, that the stream extends indefinitely far above and below the airfoil. This is in contrast to a wing-propeller combination in which both the wing and stream are three-dimensional, and the extent of the shear region is finite. The second important feature is that the stream shear is constant, so that the Joukowski transformation can be applied to the governing equations of fluid motion. This single fact makes it possible to obtain an exact potential solution to the problem.

The exact solutions for the lift, pitching moment, and pressure distribution are given in the original papers by Tsien and by Sowyrda, and will not be repeated here. It is shown in those papers that the drag of the airfoil is identically zero since the airfoil is a two-dimensional closed body in inviscid flow, and is subject to no spanwise velocity variations.

Considerable insight into the effects of shear flow on airfoil characteristics can be obtained by restricting the solutions to the case of small airfoil thickness, camber, and angle of attack. This is done for illustrative purposes to show the shear effects. The lift coefficient and moment coefficient about the airfoil midchord station are, to the first order in thickness and camber

$$C_L = \frac{L}{\rho/2 U_0^2 c} \approx 2\pi \alpha \left[1 + \gamma + \frac{\tau k_L^2}{32} \right] + 2\pi \left[\frac{\tau k_L}{4} + 2 \frac{h}{c} \left(1 + \frac{k_L^2}{32} \right) \right] \quad (1)$$

$$C_m = \frac{M}{\rho/2 U_0^2 c^2} \approx \frac{\pi}{2} \alpha \left[1 + \tau + \frac{\tau k_L^2}{16} \right] + \frac{\tau \pi k_L}{64} \quad (2)$$

where a positive pitching moment is a stalling moment, τ is the ratio of the airfoil maximum thickness to the chord, h is the maximum height of the airfoil camber line, and $k_L = \frac{c}{U_0} \frac{dU_0}{dy}$ is the local stream shear (Fig. 1).

When the shear, k_L , is taken as zero, it can be seen that Eqs. (1) and (2) reduce to the usual thick airfoil results in which the slope of the lift and moment curves are increased because of thickness. For non-zero uniform shear, it can be seen that the shear couples with both the airfoil thickness and camber to result in: (1) an increase in the slope of the lift and moment curves, much like a thickness effect, (2) an overall increase in lift at all angles of attack, analogous to a change in camber, and (3) an overall increase in pitching moment analogous to a distorted camber distribution. These changes in the airfoil characteristics are proportional to the stream shear and can be viewed as effectively associated with a distortion of the airfoil shape; that is, there is an equivalent airfoil which would exhibit these same characteristics in uniform flow. This equivalent airfoil would be thicker, have increased camber, and a different camber distribution.

It will be noted in Eqs. (1) and (2) that for small thickness and camber, the thickness and camber interactions with the stream shear are simply superimposed. The exact solution³ shows that in addition there is a coupling of thickness and camber terms which does not appear in the linearized form. In some cases this coupling term is as large as either of the other two terms. To illustrate this and the magnitude of the inviscid shear effect

on airfoils, consider a 17% thick section with 11% camber in a shear flow defined by $k = 5$. This airfoil crudely corresponds to one with about 50° flap deflection, and the shear corresponds to about the steepest velocity gradient found in a propeller slipstream. It is shown in Ref. 3 that, at zero angle of attack, with no shear, the airfoil lift coefficient is $C_L \approx 1.6$. With shear defined by $k = 5$, the lift coefficient at zero angle of attack is $C_L \approx 4.9$. The lift increment due purely to shear, $\Delta C_L \approx 3.3$, is about double that in a uniform stream due purely to camber. Moreover, each of the shear contributions due to thickness, to camber, and to coupling of thickness and camber are about the same.

Nonuniform Shear

The theory for airfoils in uniform shear flow provides considerable insight into the characteristics of airfoils in nonuniform flows. However, the elementary theoretical model of the flow bears little resemblance to that occurring in an actual propeller slipstream; in particular, the theory postulates uniform shear whereas the shear in a slipstream is markedly nonuniform. Some understanding of the influence of nonuniform shear flows on airfoil characteristics can be obtained from the two-dimensional investigations made by Jones^{4, 5}. In Ref. 4 Jones considers a thin, cambered, Joukowski airfoil in a stream with a parabolic velocity distribution given by $U_o = U_R \left[1 + \frac{q}{2} \left(\frac{y}{H} \right)^2 \right]$, where U_o , U_R , and y are defined in Fig. 2. The parameter, q , fixes the nonuniform shear, and H is the usual transformation length given approximately by

$$\frac{H}{c} \approx \frac{1}{4} (1 + \tau)$$

where c is the reference chord length and τ is the thickness chord ratio.

In contrast with the uniform shear flow problem just described, this undisturbed flow is characterized by a stream vorticity which is not constant, but varies between stream lines. From Helmholtz's law it is known that the vorticity must be conserved along a streamline, thereby implying that the disturbance stream function for a profile in this flow does not satisfy Laplace's equation. This is the fundamental difficulty in treating airfoils in nonuniform shear flow since it precludes an exact solution in closed form.

Jones' approach to the problem was to assume the airfoil thickness and camber were small, and that the stream nonuniformities were small; in particular, $g \ll 1$, $\frac{1}{2} \left(\frac{y}{H} \right)^2 \ll 1$. His approximate solutions for the airfoil lift and pitching moment about the midchord station follow after neglecting powers and products of these quantities, and are expressed as follows.

$$C_L = \frac{L}{\rho/2 U_0^2 c} \approx 2\pi\alpha \left[1 + r - g(8841 + \ln g) \right] + 4\pi \frac{h}{c} \quad (3)$$

$$C_m = \frac{L}{\rho/2 U_0^2 c^2} \approx \frac{\pi}{2} \alpha \left[1 + r - \frac{1}{2} (8730 + \ln g) \right] \quad (4)$$

In the limit of a uniform stream, these results reduce to the usual thin airfoil result with the first-order thickness correction. Additionally, these approximate solutions demonstrate another effect associated with the stream nonuniformities; that is, the slopes of both the lift curve and the pitching moment curve are increased for positive values of the shear parameter, g . To illustrate the magnitude of this effect, consider a 15% thick airfoil located at the plane of symmetry of a shear stream defined by $g \approx 1/4$

(see Fig. 2). This value of φ is the upper limit on the range of validity for the theory, and physically corresponds to a situation in which the velocity parabolically increases by about 1% in a vertical distance equal to half the airfoil thickness. This shear is modest in comparison with that occurring in propeller slipstreams. However, Eqs. (3) and (4) show that this shear results in a 20% increase in the lift curve slope and a 10% increase in the moment curve slope. A shear more typical of a propeller slipstream was experimentally investigated in previous research^{6, 7}. The shear stream used in that research was defined by $\varphi \approx 2$. Considering a 15% thick airfoil at the stream plane of symmetry, the stream velocity increases by about 7% in a vertical distance equal to half the airfoil thickness. The data reported in Refs. 6 and 7 show that the shear increased the lift curve slope by 250% over that obtained in a constant velocity stream. The conclusion is that in the two-dimensional case, nonuniform shear typical of that existing in propeller slipstreams can cause profound changes in the airfoil lift and moment characteristics.

In comparing Jones' results for an airfoil in nonuniform shear with Sowyrda's uniform shear results, it will be noted that the former does not predict any interaction of the shear with the airfoil thickness and camber to cause a camber-like increase in lift. Intuitively one would expect an interaction similar to that predicted for uniform shear since at locations removed from the stream plane of symmetry, the stream shear becomes fairly uniform. This speculation is qualitatively substantiated by a subsequent two-dimensional investigation by Jones⁵ of the forces on an elliptic cylinder in a stream with a hyperbolic distribution of velocities. These results show that, to the first order in airfoil thickness, the lift increment due to shear is given by

$$\Delta C_L = \pi/2 \ k_e \tau \quad (5)$$

where $k_e = \frac{\rho}{U} \frac{dU}{dy}$ is the shear in the undisturbed stream at the airfoil position. In addition, the experimental results reported in Refs. 6 and 7 show an overall increase in lift in nonuniform shear. In the original theoretical development for airfoils, the airfoil thickness and camber, and the stream nonuniformities are taken to be small and the products of these terms are neglected. These neglected products contain the shear interaction with the airfoil thickness and camber, and they do not appear in the final results, Eqs. (3) and (4).

The shear interaction with the airfoil thickness and camber are important for two reasons. First, the interaction results in an overall increase in lift which can be substantial. More important, the shear interaction causes an additional pressure distribution on the airfoil which would then influence boundary layer separation. The potential importance of this interaction with respect to the present problem led to a partial extension of Jones' theory⁴ to determine the effect of the shear-thickness interaction on the pressure distribution of a symmetrical airfoil. This extension is completely reported in Appendix I and will be briefly summarized here.

Appendix I follows Jones' development, but retains terms involving products of the airfoil thickness and the shear parameter, q , to obtain a partial solution. It is noted that the primary concern is with the tangential velocity distribution over the airfoil, which is comprised of a remote stream component and a disturbance component. The partial solution consists of the evaluation of the additional higher order terms in the remote stream component of the velocity.

As a check on the significance of this partial solution including the second-order terms, the results have been applied to determine the lift increment due to the thickness-shear interaction. The resulting lift increment is

$$\Delta C_L = \frac{\Delta L}{\rho/2 U_\infty^2 c} \approx \frac{8\pi}{1.3} f \tau \frac{\gamma}{c} \quad (6)$$

Defining the local stream shear as

$$k_x = \frac{c}{U} \frac{dU}{dx} \quad (7)$$

it follows that the lift increment due to the thickness-shear interaction, as given by the partial solution, is

$$\Delta C_L = \frac{\Delta L}{\rho/2 U_\infty^2 c} \approx \frac{\pi}{2} \frac{\tau k_x}{1.3} \quad (8)$$

Comparing this with the lift increment given in Eq. (1) and Eq. (5),

$\Delta C_L = \frac{\pi}{2} \tau k_x$, it can be seen that the partial solution yields about 70% of the increment predicted by uniform shear theory and other nonuniform shear theories. In addition, Eq. (8) is found to agree fairly well with the experimental data. This provides some justification for subsequently using the partial solution for the additional velocity distribution in predicting airfoil pressure distribution.

To summarize, the existing theoretical treatments for airfoils in non-uniform flows consider the two-dimensional problem in an unbounded field. In general, the treatments fall into two categories: exact solutions for airfoils in flows with uniform shear^{2, 3} and approximate solutions for airfoils in flows with symmetric nonuniform shear^{4, 5, 8}. The literature treating uniform shear flows^{2, 3} shows that the stream shear interacts with the airfoil thickness and camber to produce an overall increase in lift, much like

an increased effective camber, an overall increase in pitching moment analogous to a distorted camber distribution, and a small increase in lift and moment curve slopes analogous to an increase in airfoil thickness. The theory for thin airfoils in nonuniform shear⁴ provides an approximate solution restricted to small values of stream shear to show that the first-order effect of the nonuniform shear is to increase markedly the slope of the lift and moment curves. Since this solution neglects products of the airfoil thickness and camber with the stream shear, the shear-thickness interaction is not included. However, further work⁵ shows this interaction should be present in nonuniform shear flows, and that the magnitude of the interaction should be the same as in uniform shear. This conclusion is substantiated by experiments⁷.

EXPERIMENTS ON AIRFOIL STALL IN SHEAR FLOW

The emphasis in the experimental research has been to systematically investigate the effects of stream shear on airfoil characteristics by experimentally duplicating a flow model employed in the theoretical studies and then, progressively departing from this flow model, to approach a more practical flow situation, such as the flow in a propeller slipstream. This procedure provides a valid check on the basic theory, but, more important, allows one to isolate a number of complicating features of the physical problem. The inherent difficulty in this approach is that closely controlled shear flows must be produced in a wind tunnel.

Apparatus

The technique employed to produce shear flows in a wind tunnel is to insert nonuniform screens or grids upstream of the test section to selectively introduce losses in the stream and thereby produce a stream of nonuniform total pressure. Since the screens are nonuniform and since the velocity must be continuous through the screen, a nonuniform static pressure gradient is produced at the screen to cause flow curvature. This curvature damps out with distance from the screen because of the wall constraint, but it precludes the possibility of designing the screen by simply extrapolating the desired velocity distribution back to the screen to determine the required local screen losses.

A method for designing nonuniform screens has been reported by Owen and Zienkiewicz⁹ which is applicable for screens which perturb the flow slightly to produce a stream with a linear velocity gradient. However, the present research is concerned with large nonuniform and discontinuous shear, and it was necessary to extend that work to include these cases. This extension and the methods for constructing the screens are given in Ref. 7.

The particular screen used in the present investigation and the velocity calibration are shown in Fig. 3. The distribution of stream shear is shown in Fig. 4. This screen design was selected to produce a simulated two-dimensional propeller slipstream, and the shear within the jet is fairly typical of that behind an actual propeller. The screen was constructed

of metal rods of 1/8" to 1/2" diameter spaced in a metal frame. The view shown is the upstream side of the screen. During the flow calibration it was found that there was spottiness in the flow, evidently stemming from the rapid local expansion of the flow to an equilibrium condition before local mixing could occur. This difficulty was eliminated by bonding a fine-meshed metal honeycomb to the downstream side of the screen to locally constrain the flow and allow mixing to take place.

Calibration data are shown in Fig. 3 for the illustrated screen and are seen to agree well with the theoretical curve. The largest discrepancy occurs at the edge of the jet and reflects the effects of viscous mixing between the two streams. The flow external to the jet is seen to be somewhat nonuniform. This is ascribed to difficulties in maintaining fabrication tolerance. The screen solidity required to produce this flow is about 85%, and small deviations from the design solidity produce marked changes in the local screen losses. Since the present interests center on the shear within the jet, the small nonuniformities in the external flow are not important.

The airfoil model used in the experiments, Fig. 5, was a 17% thick symmetrical Joukowski airfoil which completely spanned the wind tunnel. In anticipation of future experiments in an axisymmetric slipstream, the model was segmented, and the center section instrumented with a three-component strain gauge balance. The model was assembled with gaps on either side of the instrumented section to prevent balance interference. The entire model was then wrapped with 0.005" thick sheet rubber to prevent flow through the gaps, and the balance was calibrated with the sheet rubber in place. The balance was designed to measure a maximum lift of about 3 pounds. During the calibration it was demonstrated that the entire system including the rubber sheet was linear to better than 0.5%, and that if these nonlinearities were included in the calibration, the balance would resolve a lift force of about 0.01 pounds.

The experiments were made in the subsonic leg¹⁰ of the CAL One-Foot High-Speed Wind Tunnel¹¹. This leg of the wind tunnel has a test section with a cross-section of 17" x 21", and is operated as a closed-throat, non-return type tunnel. It operates at atmospheric stagnation pressure over a speed range of 0 - 180 fps.

This experimental work was devoted to measuring the airfoil lift, drag, and pitching moment at various locations in the shear stream, and making observations of the airfoil boundary layer using oil film techniques. The tests were made at airspeeds of about 100 mph, and the Reynolds number based on airfoil chord length varied from 3×10^5 at the center of the stream to 6.75×10^5 near the edge of the slipstream.

Force Data

The lift and pitching moment data are presented in Figs. 6, 7, and 8. The drag data are not presented since it has been established⁷ that the artificial stream turbulence influences the viscous drag. The effects of artificial turbulence on lift will be discussed subsequently. The lift data, Figs. 6 and 7, have been reduced to coefficient form by using both the undisturbed local stream velocity and the average jet velocity. The former presentation offers a good measure of airfoil relative efficiency, while the latter provides a direct comparison of lift. The pitching moment data are reduced to coefficient form using the undisturbed local stream velocity. A scaled sketch of the airfoil and the stream velocity calibration is included in Figs. 6, 7, and 8 to show the position of the airfoil in the stream.

The angle-of-attack range covered in these experiments was not sufficient to obtain the usual indication of airfoil stall, that is, a definitive maximum in the lift curve. However, the data obtained showed, in most cases, that stall was imminent, and the figure of merit used here is the lift at which the stall process began, termed the usable maximum lift. This was identified using both the pitching moment data and the drag data. Stall begins when there are large regions of separated flow on the airfoil which grow with increasing lift. The growth of these separated flow regions is manifested by a moving center of pressure on the airfoil, and by increased drag. The criterion used with the moment data to establish the beginning of the stall process was the point at which $\partial C_m / \partial C_L = 0$. No quantitative criterion could be applied to the drag data, and a sudden increase in drag was interpreted as the beginning of stall. The lifts at which these two measurements indicate approaching stall are shown in Figs. 6 and 7, and these two criteria are seen to be in rather good agreement. It is interesting to note that these criteria also agreed well with the observed beginning of lift unsteadiness, a pilot's measure of approaching stall.

The most important property exhibited by the data in Figs. 6 and 7 is a destalling phenomenon associated with airfoil position in the stream. The data show that with the airfoil located immediately below the stream plane of symmetry ($\frac{y}{r} = -\frac{1}{16}, -\frac{1}{8}; -\frac{3}{16}$) and near the boundary of the shear stream ($\frac{y}{r} = \frac{7}{8}$), stall is delayed relative to the observed stall at other airfoil positions. The magnitude of this effect is evidenced by comparing the data obtained at $\frac{y}{r} = -\frac{1}{8}, 0$, and $+\frac{1}{8}$ with data obtained in a comparable uniform slipstream^{7*}. The stream shear and the usable maximum lift coefficients (based on average stream velocity) are summarized in Table I.

TABLE I

The Maximum Usable Lift Coefficients in Uniform and Nonuniform Streams

Stream	Model Position, $\frac{y}{r}$	Shear, k_s	Max. Lift-Coefficient
Uniform	0	0	0.70
Nonuniform	0	0	0.75
Nonuniform	-1/8	-2.07	1.10
Nonuniform	+1/8	+1.78	0.48

First, in comparing the usable maximum lift measured at the center of the uniform and nonuniform streams, it is seen that the two agree closely. The difference in lift is smaller than the errors in the corrections applied to account for the differing boundary interference. It is concluded that, for practical purposes, the usable maximum lift measured in the center of the shear stream is equivalent to that measured in the center of the comparable uniform jet.

The data obtained at $\frac{y}{r} = \pm 1/8$ in the shear stream show profound effects of stream shear on usable maximum lift. These data show that by ^{*The comparable uniform slipstream was free of velocity gradients with a velocity equal to the average velocity in the nonuniform stream considered here.} The resulting changes in airfoil lift due to the different boundary effects were computed and applied to the data to provide a valid comparison.

moving the airfoil below the stream plane of symmetry through a distance corresponding to half the airfoil maximum thickness, the usable maximum lift was increased by about 50%. Similarly, in moving the airfoil above the plane of symmetry, the lift was decreased by about 40%. The other data in Fig. 7 confirm this general trend. When the airfoil is in the vicinity of $\frac{y}{c} \approx +3/8$ to $1/2$, the usable maximum lift is comparable with that measured at the center of the stream, and finally, with airfoil near the slipstream boundary, the stall is evidently delayed.

It is interesting to compare the observed maximum lift variations with the stream shear characteristics, Fig. 4. Below the center plane, where the maximum lift is augmented, the stream shear is negative and the shear derivative is positive. At the center of the stream, where the maximum lift is unaltered, the shear is zero but its derivative is positive. Immediately above the centerplane, where the maximum lift is decreased, both the shear and its derivative are positive. At $\frac{y}{c} \approx +3/8$ to $1/2$, where the maximum lift is unaltered, the shear is a maximum but its derivative is near zero. Near the slipstream boundary ($\frac{y}{c} \approx +7/8$), where stall is evidently delayed, the shear is positive but its derivative is negative. This correlation of maximum lift with stream characteristics is summarized in Table II and plotted in Fig. 9. The data point for $\frac{y}{c} \approx 7/8$ is not plotted since it falls far off scale. The conclusion reached from this qualitative type of correlation is that the observed destalling phenomenon is associated with both the

TABLE II
Correlation of Maximum Lift with Stream Shear

Airfoil Position	Shear, k_s	Shear Derivative, k'_s	Effects on Maximum Lift	k_s k'_s
$-\frac{3}{8} \leq \frac{y}{c} < 0$	Negative	Positive	Beneficial	Negative
$\frac{y}{c} \approx 0$	0	Positive	None	0
$0 < \frac{y}{c} < \frac{3}{8}$	Positive	Positive	Detrimental	Positive
$\frac{3}{8} < \frac{y}{c} < \frac{1}{2}$	Positive	~ 0	None	~ 0
$\frac{y}{c} \approx \frac{7}{8}$	Positive	Negative	Beneficial	Negative

stream shear and its derivative, and it appears that a beneficial destalling effect is obtained when the product of the stream shear and its derivative is negative. A detrimental effect is obtained when the product is positive, and sensibly no effect is observed when either the shear or its derivative is zero.

It should be noted that apparently this same destalling phenomenon was encountered by Brenckman¹² in his wing-propeller slipstream experiment. His experiment consisted of measuring the spanwise lift distribution on a wing of infinite span intercepting an actual propeller slipstream. The wing was located so that it was nominally centered with respect to the slipstream, and it was found that the maximum lift coefficient with the slipstream was about 20% greater than in uniform flow. Brenckman observed this destalling phenomenon both inside and outside the slipstream, and ascribed the phenomenon occurring within the slipstream to be associated with a boundary layer stabilization mechanism. His experimental model precludes the possibility of associating this mechanism with the stream shear because of its three-dimensional character.

Oil Film Studies

One possible cause of the observed destalling phenomenon in the present two-dimensional experiments is the occurrence of a three-dimensional separation process with accompanying vortex formations which could energize the flow and locally delay separation on the instrumented section. As a check on this hypothesis, the complete series of experiments were rerun using oil film techniques to observe the boundary layer separation process. The aerodynamic forces were monitored during these experiments to insure that the observed phenomena corresponded to the previous results. Typical photographs of the observed separation processes are presented in Figs. 10, 11, and 12.

The photographs shown in Fig. 10 were made with the airfoil at the $\frac{y}{r} = -3/16$ position. The view is looking down on the upper surface from a point about one chord length ahead of the wing, and the flow is from the bottom to the top of the picture. Early in the original research⁷, it was found that with the wing spanning the wind tunnel, the wing at high angles of attack caused wall boundary layer separation which resulted in unusual

vortex formations on the wing. To prevent this, the side walls were perforated, and suction was applied to bleed off the wall boundary layer. The wall perforations can be seen in the photographs in Figs. 10, 11, and 12. The suction and distribution of the perforations were experimentally fixed to provide a reasonably two-dimensional separation pattern*.

The oil film technique used in these experiments was to apply oil colored with lampblack at the airfoil leading edge while the wind tunnel was running, and to observe the patterns after an equilibrium pattern had been established. A separated region is identified as a region where the oil tends to accumulate. A typical sequence of this operation is shown in Fig. 11. Photograph 6 shows the oil pattern shortly after application; photograph 7 shows the pattern after about two minutes; and photograph 8 shows the pattern at or near equilibrium. In monitoring the forces, it was found that the oil did not noticeably influence the forces at any time during the procedure, and it was concluded that the observed formations were a valid indication of boundary layer separation.

The important conclusion reached from Fig. 10 is that there was no substantial separation of the boundary layer up to an angle of attack of 12° . Several isolated separated regions can be noted in photograph 8 where the oil tends to accumulate. At $\alpha = 14.2^\circ$, these same regions are apparent, and at $\alpha = 17.3^\circ$, the oil appears to accumulate on the rear third of the wing. However, there are no regions clearly indicating flow separation.

The photographs shown in Fig. 11 were obtained with the airfoil positioned at $\frac{y}{x} = -1/8$, and a no-flow photograph is included for comparison. At $\alpha = 8.7^\circ$, it is apparent that sufficient time was not allowed to reach an equilibrium pattern, but there appear to be no regions of separated flow. The photographs taken at $\alpha = 11.9^\circ$, 14.6° , and 15.6° show five or six spots of oil accumulation, suggesting local flow separations that do not change markedly. At $\alpha = 16.4^\circ$, these regions appear to have merged, *Checks were made at small angles of attack to determine the influence of the sidewall suction on lift. It was found that the change in lift coefficient due to suction was about 0.01.

indicating a general pattern of decreased velocities at the trailing edge, but still no definite separation. The three-dimensional patterns appearing at the wing extremities are caused by improperly adjusted bleed air through the walls. Subsequent checks showed that these patterns could be eliminated without altering the general oil pattern. The photographs in Figs. 10 and 11, then, qualitatively substantiate the force data in that no strong flow separations are observed.

The photographs shown in Fig. 12 were obtained with the airfoil positioned at $\frac{y}{r} = +1/8$, a position where the force data clearly indicate the beginning of stall at $\alpha \approx 11^\circ$. A no-flow photograph is shown for comparison. Again at $\alpha = 6.3^\circ$ equilibrium oil patterns had not been fully established, but two distinct regions of separated flow are apparent. These are probably caused by some three-dimensional effect. At $\alpha = 9.3^\circ$, the separated flow is evidenced by the accumulation of oil and the clear regions near the trailing edge indicate reversed flow. The pattern is generally three-dimensional, reflecting the sensitivity of separation to very small spanwise gradients, but a fairly clear separation line is evident. At $\alpha = 12.3^\circ$, separation has moved forward to the midchord position, and there is an indication of leading edge separation and re-attachment. At $\alpha = 15.3^\circ$ and 17.3° , the oil patterns show a leading edge separation bubble with separation subsequently occurring at the quarter chord. A pair of vortices are evident, and cause the intricate flow patterns in the separated region. It is believed that the position of these vortices is influenced by wall proximity, but their existence does not appear to depend on the walls. This is substantiated by the photograph at $\alpha = 9.3^\circ$. Many of the oil accumulations indicated weak vortex formations normal to the surface. The vortex pair that subsequently formed apparently reflects the coalescing and strengthening of these distributed vortices.

To summarize, the oil film studies showed that no unusual three-dimensional separation patterns were present on the wing under conditions corresponding to destalling, and that a normal type of separation was present when stall was observed. The conclusion is that the destalling phenomenon is associated with an inviscid or viscid interaction with the nonuniform stream.

Thickness-Shear Interaction

The final item to be noted in the experimental data is the typical shear effect on airfoil lift. The data in Fig. 6 show a finite lift on the symmetrical airfoil at zero angle of attack. This effect was discussed in the previous section in connection with the theoretical treatment of airfoils in shear flow. The experimental lift increments due to shear are tabulated in Table III and are compared with that predicted by uniform shear theory^{2, 3}. The theoretical lift increments have been corrected for slipstream boundary

TABLE III

Comparison of Experimental and Theoretical Lift Increment due to Shear

y/r	k_L	$\Delta C_{L_{exp}}$	$\Delta C_L(Tsien)$	$\Delta C_L(corrected)^*$
-3/16	-2.60	-0.265	-0.695	-0.233
-1/8	-2.07	-0.205	-0.554	-0.194
-1/16	-1.15	-0.106	-0.308	-0.108
0	0	0	0	0
1/8	1.78	0.182	0.366	0.162
3/8	2.77	0.236	0.569	0.198
1/2	2.69	0.153	0.553	0.149

interference⁷ and these corrected values are also tabulated. It can be seen that the corrected theoretical lift increments are in good agreement with the experimental data. The observed discrepancies are believed to stem from the approximate methods used in accounting for the boundary proximity. Since the partial extension to Jones' theory⁴ yields substantially the same lift increment due to shear, this agreement between theory and experiment serves to verify the extension. This verification is important since the extension of Jones' theory will be used subsequently to examine the airfoil pressure distribution.

There are a number of potential explanations for the observed destalling phenomenon which can be grouped into two categories: (1) peculiarities

*Corrected for slipstream boundary interference.

associated with the experiment, and (2) effects associated with the stream shear which are manifested in the inviscid and viscous flows about the airfoil. In the first category, there are the effects of artificially induced turbulence from the shear screens which alter the airfoil boundary layer characteristics, and the effects of the slipstream boundary which cause a disturbance flow field at the airfoil. As a check on the effects of artificially large turbulence, a uniform screen made of 1/16" wire with a solidity corresponding to the average in the shear screen was mounted in the wind tunnel to produce comparable turbulence in a uniform stream. Experiments with the airfoil model showed the effect of this turbulence was to decrease the drag by about 50% and to increase the maximum lift by about 8%. The conclusion is that the turbulence does alter the maximum lift but the change is small in comparison with the observed destalling effect.

The effect of slipstream boundary interference was previously investigated⁷ by testing the symmetrical airfoil at various vertical positions in a uniform two-dimensional slipstream. These experiments showed that the maximum lift varied only by 5% when the airfoil was tested at positions varying from $\frac{x}{r} = 0$ to $3/4$. The conclusion is that the slipstream boundary interference is not important in determining airfoil maximum lift.

The direct effects associated with stream shear appear to dominate in influencing the maximum lift, that is, the inviscid effects of shear that alter the airfoil pressure distribution, and the viscous effects of shear interacting with the airfoil boundary layer. These two topics will be discussed in the next section.

INFLUENCE OF STREAM SHEAR ON BOUNDARY LAYER SEPARATION

Within the framework of the thin boundary-layer concept, there are two effects of stream shear that can influence boundary-layer separation. The first is inviscid alterations in the airfoil pressure distribution stemming from the interaction of the stream shear with the airfoil. It was demonstrated previously that the effect of uniform shear is analogous to a warped airfoil in a uniform stream, and the additional effect of nonuniform shear can be viewed as an effective increase in airfoil thickness. Both of these characteristics imply that the pressure distribution is altered in shear flow. These effects will be examined in this Section using the available theories.

The second effect is a viscous interaction between the stream shear and the boundary layer to alter the boundary-layer characteristics. This effect has been considered by a number of investigators¹³⁻¹⁶ with the emphasis on determining the changes due to stream shear in skin friction, convective heat transfer, and boundary-layer thickness with no external pressure gradient. The present problem is concerned with conditions influencing boundary-layer separation, and hence the pressure gradient must be considered. Boundary-layer theory for bodies in a uniform stream¹⁷ shows that the criterion for separation depends only on the Reynolds number and the pressure gradient. In this section the classical laminar boundary layer development will be generalized to the case of a stream with shear to determine the effects of shear on the criterion for separation.

Pressure Distribution

The experiments described were made in a stream with nonuniform shear, and consequently consideration will be restricted to the two theories that apply for nonuniform shear flow. The basic theory is that of Jones⁴ which is restricted to thin airfoils and to streams with small nonuniformities. The restriction to small stream nonuniformities precludes the calculation of a pressure distribution for stream conditions corresponding to those in the experiment. Similarly, the extension of Jones' theory (Appendix I) to retain the shear interaction with the airfoil thickness is applicable only for small stream nonuniformities. However, a theoretical calculation of the pressure distribution will demonstrate the trend of the shear effects on pressure distribution.

The distribution of velocities over the airfoil given by Jones⁴ has been linearized in angle of attack, neglecting camber effects, as follows:

$$\frac{U}{U_\infty} = \frac{1}{A} \left\{ \sum_{n=0}^3 + \alpha_n \cos n\varphi + \sum_{n=1}^3 \beta_n \sin n\varphi \right\} \quad (9)$$

where

$$\begin{aligned} \alpha_0 &= \left[\frac{2}{\sigma^2} + g \left(\frac{\gamma}{H} \right)^2 - 1.7682 g \right] \alpha \\ \alpha_1 &= \left[2 + g \left(\frac{\gamma}{H} \right)^2 - 0.2682 g - 2 \left(\frac{\sigma-1}{\sigma} \right) \right] \alpha \\ \alpha_2 &= \left[g - \frac{2(1-\sigma)}{\sigma^2} \right] \alpha \\ \alpha_3 &= -\frac{1}{2} g \alpha \\ \beta_1 &= 2 + g \left(\frac{\gamma}{H} \right)^2 \\ \beta_2 &= 2g \left(\frac{\gamma}{H} \right) \alpha \\ \beta_3 &= 0 \end{aligned} \quad (10)$$

$$A = \left[(8\kappa_0^2 - 4\kappa_0) \cos \varphi + (4\kappa_0 - 2) \cos 2\varphi + 4\kappa_0 \cos 3\varphi + 2 - 4\kappa_0 + 8\kappa_0^2 \right]^{1/2}$$

$$\kappa_0 \approx \gamma/1.3$$

$$\sigma = 1 + \frac{1}{2} g \ln g$$

and the transformation to the airfoil coordinate system is

$$\frac{\kappa}{H} = \kappa_0 + \cos \varphi + \frac{(1-\kappa_0)^2 (\kappa_0 + \cos \varphi)}{1 + \kappa_0^2 + 2\kappa_0 \cos \varphi} \quad (11)$$

The additional disturbance velocity, due to the airfoil thickness-stream shear interaction, is taken from Appendix I and linearized in angle of attack.

$$\begin{aligned} \frac{\Delta U}{U_R} = \frac{q \kappa_0}{2A} & \left\{ \alpha + 4\left(\frac{y}{H}\right) + 2\left[\alpha + \alpha\left(\frac{y}{H}\right)^2 + \frac{y}{H}\right] \cos \varphi \right. \\ & + 2\left[\alpha\left(\frac{y}{H}\right)^2 - \frac{y}{H}(1+\alpha)\right] \cos 2\varphi - 2\left(\alpha + \frac{y}{H}\right) \cos 3\varphi \\ & - \alpha \cos 4\varphi + 2\left[5\alpha \frac{y}{H} - \left(\frac{y}{H}\right)^2\right] \sin \varphi \\ & \left. - 2\left[5\alpha \frac{y}{H} - \left(\frac{y}{H}\right)^2\right] \sin 2\varphi + 2\alpha\left(\frac{y}{H}\right) \sin 3\varphi \right\} \end{aligned} \quad (12)$$

The formulas given in Eqs. (9) and (12) have been used to calculate the velocity distribution on the airfoil used in the experiments ($\tau = 0.17$). In keeping with the theoretical restriction to small nonuniformities, the calculations were made for a stream defined by $q_0 = 1/4$ with the airfoil positioned at $y/H = \pm 0.2208$. These locations correspond to the experimental airfoil positions, $y/r = \pm 1/8$, but the stream shear is about an order of magnitude smaller than that in the experiments. The calculations were made for the airfoil at a lift coefficient of 0.63 at both positions. The velocity distributions are shown in Fig. 13 and are compared with the airfoil velocity distribution at the same lift coefficient, 0.63, in uniform flow. First, it will be noted that the effects of the stream shear are, in general, to cause a "saddle-backed" distribution in that the peak velocity at the leading edge is increased and moved forward, and a velocity peak occurs at the trailing edge. In addition, by changing the airfoil position from $y/r = +1/8$ to $-1/8$, experimentally shown to be beneficial, the peak velocity at the leading edge is increased.

This behavior contradicts the experimental evidence since it shows the effect of shear is to increase the adverse velocity gradient, and hence would promote separation. The cause of this behavior is apparent in the two components of the airfoil velocity distribution; the zero-thickness component, Eq. (9), and the first-order thickness component, Eq. (12). The comparison in Fig. 13 is made at constant lift coefficient. When the airfoil is located below the stream plane of symmetry, it is acted upon by negative shear.

Referring to Eq. (8), the negative shear causes an overall decrease in lift, and hence (Eq. 12) an overall decrease in the airfoil velocity distribution. It turns out that this decrease is nearly uniform over the airfoil chord with only minor changes in the distribution.

Since the comparison is at a constant lift coefficient, the decrease in lift due to the negative shear requires that the airfoil be at a larger angle of attack when located below the stream plane of symmetry. This increases the magnitude of the zero-thickness velocity component, Eq. (9). It can be seen that with the airfoil below the stream plane of symmetry, there are two effects tending to cancel each other. The zero-thickness effect is to increase the velocities and to warp the distribution, and the first-order thickness effect is to cause an overall decrease in velocity. In this particular instance, the former dominates to cause increased peaks in the velocity distribution.

It is important to note that the distributions shown in Fig. 13 necessarily correspond to a stream with small shear. In contrast, the experiments were made in a stream with shear that was nearly an order of magnitude larger. It appears that if the experimental destalling phenomenon is to be explained on the basis of airfoil pressure distribution, it will be necessary to remove the theoretical restriction to small shear and to retain higher order shear effects. This conclusion is substantiated by the experimental data. Referring back to Table II and Fig. 9, it was noted that the qualitative nature of the destalling phenomenon suggested that the dominant parameter was the product of the local shear and the local derivative of the shear, $\gamma^2(\frac{\gamma}{H})$. Referring to Eqs. (9) and (12), it can be seen that there are no terms in the velocity distribution involving this parameter. This is a consequence of the approximations used, i.e., that powers and products of γ , $\gamma(\frac{\gamma}{H})$ and γ were negligible. Evidently theoretical treatments including the effects of large stream shear are required to check this experimental behavior.

To summarize, the approximate solutions for airfoils in nonuniform shear flows show two effects on velocity distribution due to stream shear. The first, a zero-thickness effect indicated by the average of the $\gamma/r \approx \pm 1/8$ curves in Fig. 13, is a general warping of the distribution to cause peaks at the leading and trailing edges. The second effect, the first-order thickness-

shear interaction, is largely fixed by the local stream shear both in sign and magnitude. Under conditions qualitatively corresponding to those where the destalling phenomenon was experimentally observed, the sign of the thickness effect is to decrease the velocities on the airfoil. However, this effect is more than counterbalanced by accompanying changes in the zero-thickness effect so that the net change in the velocity distribution is detrimental. The experimental results suggest the destalling phenomenon is governed by the product of local shear and the derivative of local shear, a parameter which is of higher order than those considered in the theory. It is concluded that the destalling effect cannot be identified with the existing theories which are restricted to small-stream shear, and that solutions valid for large-stream shear are required.

The Laminar Boundary Layer with External Shear

Following the thin boundary-layer approach, it is possible to use theoretical or experimental data for the inviscid pressure distribution to predict the separation on an airfoil if an appropriate separation criterion is available. Pohlhausen¹⁷ has established a criterion for bodies in uniform flow using momentum integral techniques, but the applicability of this criterion to the present problem is open to question since the effects of stream shear are not included. The momentum integral techniques will be used here, following Pohlhausen, to determine the effects of nonuniform stream shear.

The applicable boundary-layer equations for steady, incompressible, two-dimensional flow are

$$u \frac{\partial u}{\partial x} + v \frac{\partial u}{\partial y} + \frac{1}{\rho} \frac{\partial p}{\partial x} = \nu \frac{\partial^2 u}{\partial y^2} \quad (13)$$

$$\frac{\partial u}{\partial x} + \frac{\partial v}{\partial y} = 0 \quad (14)$$

where u and v are the velocity components along and normal to the surface, and x and y are coordinates parallel and normal to the surface, and ν is the kinematic viscosity.

Integrating Eq. (13) from the wall to a point, ℓ , just outside the boundary layer, the momentum equation is

$$\int_0^l u \frac{\partial u}{\partial x} dy + \int_0^l v \frac{\partial u}{\partial y} dy + \int_0^l \frac{1}{\rho} \frac{\partial p}{\partial x} dy = \nu \int_0^l \frac{\partial^2 u}{\partial y^2} dy \quad (15)$$

The second term can be integrated by parts, using Eq. (14), to arrive at the following form

$$\int_0^l 2u \frac{\partial u}{\partial x} dy - U(l) \int_0^l \frac{\partial u}{\partial x} dy + \int_0^l \frac{1}{\rho} \frac{\partial p}{\partial x} dy = \nu \left[\left(\frac{\partial u}{\partial y} \right)_{y=l} - \left(\frac{\partial u}{\partial y} \right)_{y=0} \right] \quad (16)$$

The pressure term in Eq. (16) can be evaluated by noting that the boundary-layer equations apply for the outer flow and that the pressure just outside the boundary layer is

$$\frac{1}{\rho} \frac{\partial p}{\partial x} = \nu \frac{\partial^2 U}{\partial y^2} - U \frac{\partial U}{\partial x} - v \left(\frac{\partial U}{\partial y} \right) \quad (17)$$

Assuming that the boundary layer is thin and that the pressure is invariant through the boundary layer, the pressure term in Eq. (16) can be replaced by Eq. (17). Integration of this term yields the following

$$\int_0^l \frac{1}{\rho} \frac{\partial p}{\partial x} dy = \nu \left[\left(\frac{\partial U}{\partial y} \right)_{y=l} - \left(\frac{\partial U}{\partial y} \right)_{y=0} \right] - \int_0^l U \frac{\partial U}{\partial x} dy + [U(l) - U(0)] \int_0^l \frac{\partial u}{\partial x} dy \quad (18)$$

Substituting Eq. (18) into Eq. (16), the resulting equation can be manipulated further to arrive at the following form of the momentum integral

$$\frac{\partial}{\partial x} \int_0^l u(U-u) dy + \frac{\partial U}{\partial x} \int_0^l (U-u) dy - \int_0^l [U - U(0)] \frac{\partial u}{\partial x} dy = \nu \left[\left(\frac{\partial u}{\partial y} \right)_{y=l} - \left(\frac{\partial u}{\partial y} \right)_{y=0} \right] \quad (19)$$

It can be seen that Eq. (19) is similar to the classical momentum integral, but two additional terms are introduced by the stream nonuniformity; the third term on the left and the second term on the right. The magnitude of each of these terms is fixed by the shear in the external stream. If the stream shear is small in comparison with the shear in the boundary layer, these two additional terms can be neglected in comparison with the remaining terms. In the present experiments, the stream shear was about 3% of the boundary-layer shear. Hence, for present purposes, the applicable momentum integral is the classical relation.

$$\frac{\partial}{\partial x} \int_0^\infty u(U-u) dy + \frac{\partial U}{\partial x} \int_0^\infty (U-u) dy = \nu \left(\frac{\partial u}{\partial y} \right)_{y=0} \quad (20)$$

The first two integrals in Eq. (20) are identical to the classical definitions of the momentum and displacement thickness, thereby suggesting that these definitions would be applicable in nonuniform flows. The displacement thickness used here is defined in the usual manner.

$$\int_0^{\delta^*} U dy = \int_0^{\infty} (U-u) dy \quad (21)$$

Similarly, the momentum thickness is defined as

$$\int_0^{\theta} U^2 dy = \int_0^{\infty} u(U-u) dy \quad (22)$$

The present problem is to investigate the effects of a stream with a parabolic distribution of velocities. In this connection, consider a flow with the velocity distribution given by

$$U = U_0 \left[1 + \frac{q}{2} \left(\frac{y+\epsilon}{H} \right)^2 \right] \quad (23)$$

This is the same external flow considered by Jones⁴, but the coordinate y is now referred to the surface of the body.

The flow model is illustrated in Fig. 14, and since the external inviscid flow has been effectively displaced by the displacement thickness, the equivalent inviscid flow over the surface is

$$U = U_0 \left[1 + \frac{q}{2} \left(\frac{y+\epsilon-\delta^*}{H} \right)^2 \right] \quad (24)$$

Using this inviscid velocity distribution in Eqs. (21) and (22), the displacement and momentum thickness are given by the following relations

$$\delta^* \left[1 + \frac{q}{2} \left(\frac{\epsilon^2}{H^2} - \frac{\epsilon}{H} \frac{\delta^*}{H} + \frac{1}{3} \frac{\delta^{*2}}{H^2} \right) \right] = \frac{1}{U_0} \int_0^{\infty} (U-u) dy \quad (25)$$

$$\begin{aligned} \theta \left\{ 1 + q \left[\left(\frac{\epsilon-\delta^*}{H} \right)^2 + \left(\frac{\epsilon-\delta^*}{H} \right) \frac{\theta}{H} + \frac{1}{3} \left(\frac{\theta}{H} \right)^2 \right] \right. \\ \left. + \left(\frac{q}{2} \right)^2 \left[\left(\frac{\epsilon-\delta^*}{H} \right)^4 + 2 \frac{\theta}{H} \left(\frac{\epsilon-\delta^*}{H} \right)^3 + 2 \left(\frac{\theta}{H} \right)^2 \left(\frac{\epsilon-\delta^*}{H} \right)^2 \right. \right. \\ \left. \left. + \left(\frac{\theta}{H} \right)^3 \left(\frac{\epsilon-\delta^*}{H} \right) + \frac{1}{5} \left(\frac{\theta}{H} \right)^4 \right] \right\} = \frac{1}{U_0^2} \int_0^{\infty} u(U-u) dy \end{aligned} \quad (26)$$

In the limit of uniform external flow ($g = 0$), these relations are reduced to the usual expressions for the displacement and momentum thickness. By retaining the classical definitions of displacement and momentum thicknesses for flows with external stream shear, the relations have been considerably complicated in that the equations are cubic and quintic in the thickness.

Following the Pohlhausen approach, it is assumed that the boundary-layer profile is adequately represented by a quartic series expansion

$$u = U_0 \left[1 + \frac{g}{2} \left(\frac{\delta + \epsilon - \delta^*}{H} \right)^2 \right] f(\eta) \quad (27)$$

$$f(\eta) = a\eta + b\eta^2 + c\eta^3 + d\eta^4$$

where $\eta = y/\delta^*$, δ is the boundary-layer thickness, and a, b, c , and d are free constants to be determined from the boundary conditions. The appropriate boundary conditions are

$$\text{At } y = 0: \quad u = v = 0$$

$$v \frac{\partial^2 u}{\partial y^2} = -u \frac{\partial v}{\partial x}$$

$$\text{At } y = \delta:$$

$$u = U = U_0 \left[1 + \frac{g}{2} \left(\frac{\delta + \epsilon - \delta^*}{H} \right)^2 \right]$$

$$\frac{\partial u}{\partial y} = \frac{\partial U}{\partial y} = U_0 g \left(\frac{\delta + \epsilon - \delta^*}{H^2} \right)$$

$$\frac{\partial^2 u}{\partial y^2} = \frac{\partial^2 U}{\partial y^2} = \frac{U_0 g}{H^2}$$

Applying these boundary conditions to Eq. (27) the velocity profile is determined.

$$u = U_0 \left[1 + \frac{g}{2} \left(\frac{\delta + \epsilon - \delta^*}{H} \right)^2 \right] \left[F(\eta) + \Lambda G(\eta) + \lambda H(\eta) + \xi I(\eta) \right] \quad (28)$$

where

$$\Lambda = \frac{\delta^2}{\nu} \frac{\partial u}{\partial x}$$

$$\lambda = \frac{\frac{g \delta^2}{2 H^2}}{1 + \frac{g}{2} \left(\frac{\epsilon + \delta - \delta^*}{H} \right)^2}$$

$$\xi = \frac{\frac{g}{2} \frac{\delta}{H} \left(\frac{\epsilon - \delta^*}{H} \right)}{1 + \frac{g}{2} \left(\frac{\epsilon + \delta - \delta^*}{H} \right)^2}$$

and

$$F(\eta) = 2\eta - 2\eta^3 + \eta^4$$

$$G(\eta) = \frac{1}{6}(\eta - 3\eta^2 + 3\eta^3 - \eta^4)$$

$$H(\eta) = \frac{1}{3}(-5\eta + 9\eta^3 - 4\eta^4)$$

$$I(\eta) = 2(-\eta + 2\eta^3 - \eta^4)$$

The parameter, Λ , in Eq. (28) is the familiar Pohlhausen shape factor which expresses the influence of pressure gradient on boundary-layer development. In the limit of a uniform stream, $g \rightarrow 0$, Eq. (28) reduces to Pohlhausen's result. The effects of the stream shear are introduced through two additional shape factors, λ and ξ . Noting that the denominator in these two parameters is simply U_s/U_o , where U_o is the velocity at the outer edge of the boundary layer, it can be seen that the sum of these two shape factors can be regarded as a "shear number" or "vorticity number". That is, a measure of the shear in the boundary layer is U_s/δ . The shear at the edge of the boundary layer is $\frac{g U_o}{H} \left(\frac{\delta + \epsilon - \delta^*}{H} \right)$. Since

$$\lambda + \xi = \frac{\frac{g U_o}{2 H} \left(\frac{\delta + \epsilon - \delta^*}{H} \right)}{U_o/\delta}$$

it follows that this sum is the ratio of the free stream shear to the boundary-layer shear. The fact that these two parameters do not appear as a simple pair implies that the pertinent stream shear is not that at the edge of the boundary layer, but rather some average value.

Using the results of Eqs. (25), (26), and (27), the momentum and displacement thickness can be written down immediately

$$\frac{\delta^*}{\delta} \left[1 - \lambda - 2\xi + \xi \left(\frac{\delta^*}{\delta} \right) + \frac{\lambda}{3} \left(\frac{\delta^*}{\delta} \right)^2 \right] = \frac{3}{10} - \frac{\Lambda}{120} - \frac{19\lambda}{60} - \frac{3}{5} \xi \quad (29)$$

$$\begin{aligned} \frac{\theta}{\delta} \left[(1 - \lambda - 2\xi)^2 + 2\xi (1 - \lambda - 2\xi) \left(\frac{\theta}{\delta} \right) + \frac{2}{3} \lambda (1 - \lambda - 2\xi + \frac{2\xi^2}{\lambda}) \left(\frac{\theta}{\delta} \right)^2 \right. \\ \left. + \lambda \xi \left(\frac{\theta}{\delta} \right)^3 + \frac{\lambda^2}{5} \left(\frac{\theta}{\delta} \right)^4 \right] \end{aligned} \quad (30)$$

$$= \frac{37}{315} - \frac{\Lambda}{945} - \frac{\Lambda^2}{9072} + \frac{64}{105} \lambda - \frac{106}{315} \xi + \frac{286}{2835} \lambda^2$$

$$+ \frac{64}{315} \xi^2 - \frac{13\lambda\Lambda}{22680} - \frac{13\xi\Lambda}{3780} + \frac{533}{1890} \lambda \xi$$

These formulas also are reduced to Pohlhausen's results in the limit of vanishing stream shear ($\lambda = \xi = 0$).

The important consideration in the present problem is the criterion for separation. Separation occurs when the shear at the surface vanishes. Applying this condition to Eq. (28), it follows that separation occurs when the following criterion is met.

$$\Lambda \geq -12 + 10\lambda + 12\xi \quad (32)$$

It is possible to combine the relations for the momentum and displacement thicknesses, Eqs. (25) and (26), with the momentum integral, Eq. (20), and cast the resulting differential equation into a form that can be solved, using Eq. (31), to predict separation. This procedure, in the case of a uniform external flow, is feasible because of the elementary form of the relations for the momentum and displacement thicknesses and because the velocity profile can be represented by a single parameter. The complicating feature when the external flow is nonuniform is that the expressions for the momentum and displacement thicknesses involve powers of the thicknesses, and so result in a complicated nonlinear differential equation. Numerical methods could be used to solve the differential equation; however, considerable

understanding of shear phenomena can be obtained from elementary considerations.

The approach taken here is to use a linear approximation for the momentum and displacement thicknesses in an approximate calculation following that of Prandtl¹⁸. This approach is used, not to arrive at a quantitative criterion, but to determine the qualitative effects of stream shear on separation.

Taking the displacement and momentum thicknesses to be small in comparison with the wing chord, Eqs. (25) and (26), to the first order in $\frac{\delta^*}{H}$ and $\frac{\theta}{H}$, reduce to

$$\delta^* U_\delta \approx \int_0^\infty (U-u) dy \quad (33)$$

$$\theta U_\delta^2 \approx \int_0^\infty u(U-u) dy \quad (34)$$

Inserting these relations in Eq. (20), the momentum equation becomes

$$\frac{\partial}{\partial x} [U_\delta^2 \theta] + \delta^* U_\delta \frac{\partial U_\delta}{\partial x} = \nu \left(\frac{\partial u}{\partial y} \right)_{y=0} \quad (35)$$

Substituting for the surface shear terms using Eqs. (24) and (27) and rearranging terms, Eq. (35) can be reduced to the following form

$$\frac{U_\delta \theta}{\nu} \frac{d\theta}{dx} = \frac{\theta}{\delta} \left[2 + \frac{\Lambda}{6} - \frac{5\lambda}{3} - 2\xi \right] - \left(2 + \frac{\delta^*}{\theta} \right) \left(\frac{\theta}{\delta} \right)^2 \Lambda \quad (36)$$

Following Prandtl's argument, it is assumed that the boundary layer is acted upon by the inviscid pressure distribution up to a point which is close to separation. Starting at this point, it is assumed that the pressure gradient is such that the shape of the velocity profile remains unchanged further downstream; that is, the shape factor, Λ , is a constant from this point on. By definition,

$$\frac{\theta^2}{\nu} = \Lambda \left(\frac{\theta}{\delta} \right)^2 \frac{1}{\frac{dU}{dx}}$$

and after differentiation

$$\frac{\theta}{\nu} \frac{d\theta}{dx} = -\frac{\Lambda}{2} \left(\frac{\theta}{\delta} \right)^2 \frac{U_\delta''}{(U_\delta')^2} \quad (37)$$

where the primed symbols denoted differentiation with respect to the x-coordinate. Substituting Eq. (37) into Eq. (36) and rearranging terms, the following relation is obtained

$$\frac{U_\delta U_\delta''}{(U_\delta')^2} = 2\left(2 + \frac{\delta^*}{\theta}\right) - \frac{2}{\Lambda \frac{\theta}{\delta}} \left[2 + \frac{\Lambda}{6} - \frac{5\lambda}{3} - 2\xi\right] \quad (38)$$

Using Eq. (38) and the preceding assumptions as to the boundary-layer characteristics near separation, a velocity criterion can be established for preventing separation. Prandtl does this by assigning a value to the shape factor, $\Lambda = -10$, which is near the value for separation. The equivalent procedure here is to take

$$\Lambda = -10 + 10\lambda + 12\xi \quad (39)$$

Substituting this value into Eq. (38), the criterion for just preventing separation is

$$\frac{U_\delta U_\delta''}{(U_\delta')^2} > 2\left(2 + \frac{\delta^*}{\theta}\right) + \frac{2}{\theta/\delta} \left[\frac{\frac{1}{3}}{10 - 10\lambda - 12\xi}\right] \quad (40)$$

This criterion is reduced to that of Prandtl in the limit of vanishing stream shear, $\lambda = \xi = 0$. The significance of this criterion is unchanged. That is, separation can be delayed if the second derivative of the velocity is sufficiently large and is positive. Indeed, a prerequisite for preventing separation is that U_δ'' be positive. If it is positive and if the product $U_\delta U_\delta''$ is large in comparison with the velocity gradient term, $(U_\delta')^2$, separation can be delayed.

Some insight into the significance of the shear in altering the criterion for separation can be obtained by assigning numerical values to the shape factors, λ and ξ . The values used here correspond to the properties of the shear stream generated in the experiments with the airfoil located at $y/r = \pm 1/8$. For purposes of comparison, the case of a uniform stream is included. The displacement and momentum thicknesses were calculated using only the first-order terms in Eqs. (29) and (30) and are summarized in Table IV.

TABLE IV

The Effects of Stream Shear on the Separation Criterion

$\frac{\gamma}{r}$	λ	ξ	$\frac{\delta^*}{\delta}$	$\frac{\theta}{\delta}$	$\frac{\delta^*}{\theta}$	Δ	$\left[\frac{U_\delta U_\delta''}{(U_\delta')^2} \right]_{MIN.}$
	0	0	0.383	0.117	3.28	-10	11.13
+1/8	0.01	0.03	0.386	0.128	3.01	-9.54	10.57
-1/8	0.01	-0.03	0.381	0.117	3.26	-10.26	11.08

The data in Table IV demonstrate the effect of shear on two criteria for separation. One criterion is that previously derived, the pressure gradient, Δ , at separation. Eq. (32) and Table IV show that the parameter, $+\lambda$, is always detrimental and promotes separation. However, the parameter, ξ , can take on a negative sign, corresponding to the experiments below the stream plane of symmetry, and in this case separation is delayed.

In contrast the criterion on $\frac{U_\delta U_\delta''}{(U_\delta')^2}$ shows that positive λ and ξ are beneficial in that a wider range of velocity gradients is permissible. For positive λ and negative ξ , the conditions under which the de-stalling phenomenon was observed, the criterion for separation is nearly identical to that for a uniform stream.

The conclusion is that stream shear can alter the criteria for boundary-layer separation, but under conditions corresponding to those in the experiments, these alterations are negligibly small and the uniform stream criteria apply.

CONCLUDING REMARKS

In summary, the two-dimensional experiments made with an airfoil in a symmetric nonuniform shear flow disclosed that under conditions when the product of the local shear and the local derivative of shear was negative, airfoil stall was markedly delayed. When this product was positive, stall was promoted. Subsequent experiments served to eliminate extraneous experimental factors as the cause of this phenomenon and, by elimination, to isolate the cause as stemming from inviscid alterations in the airfoil pressure distribution and/or changes in the criterion for boundary-layer separation.

A Pohlhausen calculation of the laminar boundary layer with a non-uniform external stream disclosed that the external shear tends to alter a criterion for separation. However, a numerical example showed that in the experiments, this effect would be negligibly small, leading to the conclusion that shear effects to alter the boundary-layer characteristics were not the source of the destalling phenomenon.

The available approximate airfoil theories were applied to the present problem to determine the effects of shear on the distribution of velocities over the airfoil. Since the theories are restricted to small stream shear (an order of magnitude smaller than the experimental conditions), it was not possible to calculate the distributions under stream conditions duplicating those in the experiments. However, the calculations showed two effects tending to counterbalance each other. The zero-thickness shear effect is to cause a "saddle-backed" distribution, while the first-order shear-thickness interaction tends to cause an overall decrease in velocity on the airfoil under conditions similar to those in which delayed stall was observed. Since the former is larger than the latter effect, within the limits of the theory, stall should be promoted.

It is noted that parametric dependence of the destalling effect deduced from the experimental results (that the product of the local shear and the derivative of the local shear be negative) is of higher order than covered by either theory, and it is concluded that a theory valid for large values of stream shear is required to check the experimental results.

With this qualitative understanding of the cause of the destalling phenomenon, it is possible to speculate on a number of practical applications that can be used to augment wing maximum lift. The most obvious application is to exploit the shear inherent in propeller-driven aircraft by properly orienting the wing with respect to the slipstream axis, that is, the wing somewhat below the slipstream axis. This application might be particularly effective in deflected slipstream configurations in which the wing is almost entirely immersed in a shear flow. The practicability of this scheme is qualitatively demonstrated by Brenckman's experimental results¹² and by more recent CAL experimental results¹⁹. Both show that the destalling phenomenon is realized with axisymmetric slipstreams.

Another potential means for utilizing the destalling phenomenon associated with shear flows is to artificially generate a shear flow ahead of a wing. Previous experimental research disclosed that stall is essentially unaffected in two-dimensional flow by the proximity of the slipstream boundary. This suggests that a fairly thin shear flow, perhaps comparable in thickness to the airfoil thickness, might suffice to delay stall. Since this is of interest only at very low speeds, the shear could be generated with nonuniform screens, as in the experiments. There would be a drag penalty since losses are being introduced, but the losses are purely viscous and vary as the square of the velocity, so that they might be made small. Alternatively, the shear could be generated with air jets spanning the wing. Again, these would be employed only at low speeds so that the required power might not be prohibitive.

APPENDIX

THE THICKNESS-SHEAR INTERACTION IN NONUNIFORM SHEAR FLOW

A potential explanation of the destalling phenomenon observed in the experiments with an airfoil in nonuniform shear flow is that the stream shear causes alterations in the airfoil pressure distribution. This possibility was investigated by using the available theory⁴ to calculate airfoil pressure distributions under conditions similar to those in the experiments. That is, the distributions were calculated for the airfoil located above and below the stream plane of symmetry, where the experiments showed stall should be promoted and delayed, respectively. The calculations showed the two pressure distributions were nearly identical and suggested stall should occur at the same lift regardless of location in the stream.

It was noted that the theory⁴ was approximate in that the stream shear and airfoil thickness were assumed small, and products of the airfoil thickness and the stream shear parameters were neglected. The experimental data show there is a sizable thickness-shear interaction, and it was suggested that by retaining these terms in the theoretical pressure distribution, the destalling effect might be explained. This led to the following extension of Jones' theory to predict the thickness-shear interaction.

In a flow with shear, the stream function is governed by the equation

$$\nabla^2 \psi = f(\psi) \quad (\text{I-1})$$

where f is an unknown function. If we take the distribution of velocities in the remote stream to be

$$U = -V \left(1 + \frac{q}{2} \frac{Y^2}{H^2} \right) \quad (\text{I-2})$$

the corresponding stream function is

$$\psi = -V \left(Y + \frac{q Y^3}{6 H^2} \right) \quad (\text{I-3})$$

Introducing a perturbation stream function ψ_1 to describe the flow deviation due to the airfoil, we find, to the first order in g , that

$$\Delta^2 \psi_1 = \frac{g}{H^2} \psi_1 \quad (I-4)$$

Equation (I-4) is to be solved subject to the boundary condition

$$\psi = \psi_0 + \psi_1 = \text{constant on airfoil surface.} \quad (I-5)$$

The boundary value problem specified by (I-4) and (I-5) is now attacked in the usual way.* As a first step, the equations are transformed to a coordinate system aligned with the airfoil by use of the relations

$$\left. \begin{aligned} X &= x \cos \alpha - y \sin \alpha \\ Y &= \epsilon + x \sin \alpha + y \cos \alpha \end{aligned} \right\} \quad (I-6)$$

The geometric parameters ϵ and α are respectively the distance above the axis of symmetry of the incident flow and the angle of attack. The second step is to specify the airfoil as that mapping in the x - y plane from the circle $\xi = 0$ by the conformal transformation

$$Z = x + iy = Z_0 + H e^{(\xi + i\varphi)} + \frac{(H - x_0)^2}{Z_0 + H e^{(\xi + i\varphi)}} \quad (I-7)$$

or

$$Z \simeq Z_0 + H e^{(\xi + i\varphi)} + (H - 2x_0) e^{-(\xi + i\varphi)} - Z_0 e^{-2(\xi + i\varphi)}, \quad (I-8)$$

which is correct to the first order in x_0 and y_0 . The geometrical parameters introduced in Eq. (I-8) have the following significance: x_0 and y_0 are, of course, the coordinates of the circle of radius H which transforms into the airfoil, but in addition, y_0/H specifies the camber of the wing. For a symmetrical airfoil $y_0/H = 0$ and the thickness is a unique function of x_0/H , which for small values of x_0/H is approximately linear.

Under the transformations (I-6) and (I-8), the field equation (I-4) becomes

$$\frac{\partial^2 \psi_1}{\partial \xi^2} + \frac{\partial^2 \psi_1}{\partial \varphi^2} = 2g \left\{ (\cosh 2\xi - \cos 2\varphi) - \frac{2\kappa_0}{H} \left(e^{-2\xi} - e^{-\xi} \cos 3\varphi + e^{-3\xi} \cos \varphi \right) \right\} \psi_1(\xi, \varphi), \quad (I-9)$$

while after considerable manipulation, the boundary condition reduces to

$$\psi_1(0, \varphi) + \sum_{n=0}^4 (\mu_n(0) \cos n\varphi + \nu_n(0) \sin n\varphi) = C = \text{constant} \quad (I-10)$$

The boundary value problem specified by (I-9) and (I-10) is difficult since Eq. (I-9) is, as it stands, inseparable. E. E. Jones, in Ref. 4, suggested the neglect of the terms in $g\kappa_0$, which reduces the problem to the partial differential equation of Mathieu²⁰. It is probably possible to regard Jones' solution as the zero-order approximation and proceed by perturbation theory, obtaining the equations

$$\left[\frac{\partial^2}{\partial \xi^2} + \frac{\partial^2}{\partial \varphi^2} + 2g (\cos 2\varphi - \cosh 2\xi) \right] \psi_{1,n+1} = -\frac{4}{H} \left[e^{-2\xi} - e^{-\xi} \cos 3\varphi + e^{-3\xi} \cos \varphi \right] \psi_{1,n} \quad (I-11)$$

for the subsequent stages in the iteration. Equation (I-11) is certainly easier than (I-9), but still presents some puzzling features. The form of Eq. (I-11), together with the orthonormal character of the Mathieu functions, suggests some adaptation of the perturbation procedure of quantum mechanics.

While this boundary value problem must be solved at least approximately if complete information on the effect of the $g\kappa_0$ terms is to be obtained, some information can be obtained without.

Actually, the complete solution of the extended boundary value problem, though useful, may not be essential for our immediate purpose. Both the lift and the separation point depend on the tangential velocity at the surface of the airfoil. This tangential velocity is

$$\frac{U}{V} = \frac{1}{A(\varphi)} \left(\frac{\partial \psi_0}{\partial \xi} + \frac{\partial \psi_1}{\partial \xi} \right)_{\xi=0} \quad (I-12)$$

where $A(\varphi) \equiv \left| \frac{dz}{d\xi} \right|$ is completely independent of φ . Now, under the transformations (I-6) and (I-8), the incident stream function becomes

$$\psi_0 = -V \left[\mathcal{L}(\xi, \varphi, \alpha) + \mathcal{M}(\xi, \varphi, \alpha) \kappa_0 + \frac{\varphi \mathcal{L}^3}{6H^2} + \frac{\mathcal{M} \mathcal{L}^2}{2} \left(\frac{\varphi \kappa_0}{H^2} \right) \right] \quad (\text{I-13})$$

where

$$\left. \begin{aligned} \mathcal{M} &\equiv (2e^{-\xi} \sin \varphi + e^{-2\xi} \sin 2\varphi) \cos \alpha + (1 - 2e^{-\xi} \cos \varphi - e^{-2\xi} \cos 2\varphi) \sin \alpha \\ \mathcal{L} &\equiv \epsilon + 2H \cosh \xi \cos \varphi \sin \alpha + 2H \sinh \xi \sin \varphi \cos \alpha \end{aligned} \right\} \quad (\text{I-14})$$

Consequently, the thickness effect, $\varphi \kappa_0$, is seen to enter both terms of Eq. (I-12). E. E. Jones, in Ref. 4, neglected the last term in (I-13) as being of second order in small quantities, $\varphi \kappa_0$. If we are to include this term we must add an increment

$$\Delta U = -\frac{\varphi \kappa_0}{2H^2} \frac{V}{A(\varphi)} \left[\mathcal{L}^2 \frac{\partial \mathcal{M}}{\partial \xi} + 2 \left(\mathcal{M} \mathcal{L} \frac{\partial \mathcal{L}}{\partial \xi} \right) \right]_{\xi=0} \quad (\text{I-15})$$

to the tangential velocity

$$U = \frac{1}{A(\varphi)} \left[\alpha_0 + 2 \sum_{k=1}^4 (a_k \cos k\varphi - b_k \sin k\varphi) \right] \quad (\text{I-16})$$

computed by Jones. A tedious calculation shows that the velocity increment can be expressed as

$$\Delta U = \frac{1}{A(\varphi)} \left[\delta_0 + 2 \sum_{k=1}^4 \delta_k \cos k\varphi + \beta_k \sin k\varphi \right] \quad (\text{I-17})$$

where

$$\begin{aligned}
\delta_0 &= \left(\frac{1}{4} \sin \alpha + \frac{\epsilon}{2H} \right) (\cos^2 \alpha + 1) g \kappa_0 V \\
\delta_1 &= \left[(3 + \cos^2 \alpha) \frac{\sin \alpha}{4} + \frac{\epsilon^2}{H^2} \sin \alpha + \frac{\epsilon}{H} \right] g \kappa_0 V \\
\delta_2 &= \left[\frac{1}{2} \sin^2 \alpha + \frac{\epsilon^2}{H^2} \sin \alpha + \frac{\epsilon}{H} (2 \sin^2 \alpha - \sin \alpha \cos^2 \alpha - \cos^2 \alpha) \right] g \kappa_0 V \\
\delta_3 &= \left[\frac{5}{4} \sin^3 \alpha - \sin \alpha - \frac{\epsilon}{H} \cos 2\alpha \right] g \kappa_0 V \\
\delta_4 &= \left[\frac{3}{4} \sin^3 \alpha - \frac{2}{4} \sin \alpha \right] g \kappa_0 V \\
\beta_1 &= \left[\frac{5}{2} \frac{\epsilon}{H} \sin 2\alpha - \frac{7}{4} \cos \alpha \sin^2 \alpha - \frac{\epsilon^2}{H^2} \cos \alpha \right] g \kappa_0 V \\
\beta_2 &= \left[\frac{3}{2} \sin^2 \alpha \cos \alpha - 5 \frac{\epsilon}{H} \sin \alpha \cos \alpha - \frac{\epsilon^2}{H^2} \cos \alpha \right] g \kappa_0 V \\
\beta_3 &= \left[\frac{5}{4} \sin^2 \alpha \cos \alpha + \frac{\epsilon}{H} \sin \alpha \cos \alpha \right] g \kappa_0 V \\
\beta_4 &= \left[-\frac{3}{4} \cos \alpha \sin^2 \alpha \right] g \kappa_0 V
\end{aligned} \tag{I-18}$$

Now, as Jones remarks in Ref. 4, the circulation around the airfoil is just 2π times the constant term or, in our case, $2\pi (\alpha_0 - g \kappa_0 \delta_0)$ and this circulation must be adjusted by varying an arbitrary factor in α_0 to make the velocity finite at the trailing edge of the contour. In this way, the circulation and, hence, the lift is seen to receive a contribution from $g \kappa_0$. As a matter of fact, a repetition of the argument in Ref. 4 leads to the conclusion

$$L = \frac{2\pi\rho}{H} \left\{ \begin{aligned} & \left[(a_0 - \delta_0)(a_1 - \delta_1 + a_3 - \delta_3) + 2(a_1 - \delta_1)(a_2 - \delta_2) \right] \sin \alpha \\ & + \left[(a_0 - \delta_0)(b_1 - \beta_1 + b_3 - \beta_3) + 2(a_1 - \delta_1)(b_2 - \beta_2) \right] \cos \alpha \end{aligned} \right\} \quad (I-19)$$

The significance of Eq. (I-19) is most readily determined by examining the case of zero incidence ($\alpha = 0$). According to Ref. 4

$$a_0(0) = a_1(0) = a_2(0) = a_3(0) = b_2(0) = b_3(0) = 0$$

$$b_1(0) = -V \left(2H + \frac{g^2 \epsilon^2}{H} \right) \quad (I-20)$$

while, according to Eq. (I-18)

$$\begin{aligned} \delta_0(0) &= \frac{2\epsilon}{H} g^2 \kappa_0 V & \delta_1(0) &= \frac{\epsilon}{H} g^2 \kappa_0 V \\ \beta_1(0) &= -\frac{\epsilon^2}{H^2} g^2 \kappa_0 V & \beta_2(0) &= \frac{\epsilon^2}{H^2} g^2 \kappa_0 V \end{aligned} \quad (I-21)$$

$$\beta_3(0) = 0$$

Thus, the lift increment at zero angle of attack is

$$\Delta L = \frac{2\pi\rho}{H} \left[-\delta_0(b_1 - \beta_1) + 2\delta_1\beta_2 \right]$$

or

$$\frac{\Delta L}{\rho V^2} \approx + \frac{4\pi g^2 \kappa_0 \epsilon}{H} + O\left(g^2 \frac{\epsilon^3}{H^2}\right) + O\left(\frac{g^2 \kappa_0^2}{H^2}\right) \quad (I-22)$$

REFERENCES

1. v. Sanden, H., "Über den Auftrieb im natürlichen Winde. Zeitschrift f. Math. u. Phys., 61, 225, 1912
2. Tsien, H. S., Symmetric Joukowski Airfoils in Shear Flow. Quart. of Applied Math., Vol. 1, pp. 130-148, 1943
3. Sowyrda, A., Theory of Cambered Joukowski Airfoils in Shear Flow. Cornell Aeronautical Laboratory Report No. AI-1190-A-2, September 1958
4. Jones, E. E., The Forces on a Thin Aerofoil in Slightly Parabolic Shear Flow. Z. Angew. Math. Mech., Vol. 37, pp. 362-370, 1957
5. Jones, E. E., The Elliptic Cylinder in a Shear Flow with Hyperbolic Velocity Profile. Quart. Jour. Mech. Appl. Math., Vol. X, Pt. 1, pp. 13-23, February 1957
6. Vidal, R. J., Sowyrda, A., and Hartunian, R. A., The Aerodynamic Appraisal of STOL/VTOL Configurations. Cornell Aeronautical Laboratory Report No. AI-1190-A-4, June 1960
7. Vidal, R. J., Hilton, J. H., and Curtis, J. T., The Two-Dimensional Effects of Slipstream Shear on Airfoil Characteristics. Cornell Aeronautical Laboratory Report No. AI-1190-A-5, September 1960
8. Vidal, R. J., The Influence of Two-Dimensional Stream Shear on Airfoil Maximum Lift. Presented at the IAS/ARS Joint Meeting, Los Angeles, Paper No. 61-120-1814, June 1961.
9. Owen, P. R. and Zienkiewicz, H. K., The Production of Uniform Shear Flow in a Wind Tunnel. Jour. Fluid Mech., Vol. 2, Pt. 6, pp. 521-531, August 1957
10. Vidal, R. J., Research on Rotating Stall in Axial Flow Compressors, Part III, Experiments on Laminar Separation from a Moving Wall. Cornell Aeronautical Laboratory Report No. AM-1076-A-3, January 1959
11. Wilder, J. G., Hindersinn, K., and Weatherston, R., Design of an Air Supply System and Test Section for Research on Scavenging Systems for Propulsion Wind Tunnels. WADC TR 56-6, December 1955

12. Brenckman, M., Experimental Investigation of the Aerodynamics of a Wing in a Slipstream. Jour. Aero.Sci., Vol. 25, No. 5, pp. 324-328, May 1958 (Also UTIA Tech. Note No. 11, April 1957)
13. Li, T. Y. Simple Shear Flow Past a Flat Plate in an Incompressible Fluid of Small Viscosity. Jour. Aero.Sci., Vol. 22, No. 9, pp. 651-652, September 1955
14. Glauert, M. B., The Boundary Layer in Simple Shear Flow Past a Flat Plate. Jour. Inst. Aero. Sci., Vol. 24, No. 11, pp. 848-849, Nov. 1957
15. Ting, R., Boundary Layer Over a Flat Plate in Presence of Shear Flow. Physics of Fluids, pp. 78-82, January-February 1960
16. Yen, K. T., Approximate Solutions of the Incompressible Laminar Boundary Layer Equations for a Flat Plate in Shear Flow. Jour. Aero. Sci., Vol. 22, No. 10, pp. 728-729, October 1955
17. Pohlhausen, K., Zurnaherungsweisen Integration der Differentialgleichung der laminaren Reibungsschicht. ZAMM 1, 252 (1921)
18. Prandtl, L., The Mechanics of Viscous Fluids. W. F. Durand, Aerodynamics Theory, Vol. III, p. 112, 1935
19. Vidal, R. J. and Hilton, J. H., The Effects of Slipstream Shear on Airfoil Characteristics. (To be published)
20. Whittaker, E. T. and Watson, G. N., "A Course of Modern Analysis." New York, 1943. pp. 404-416

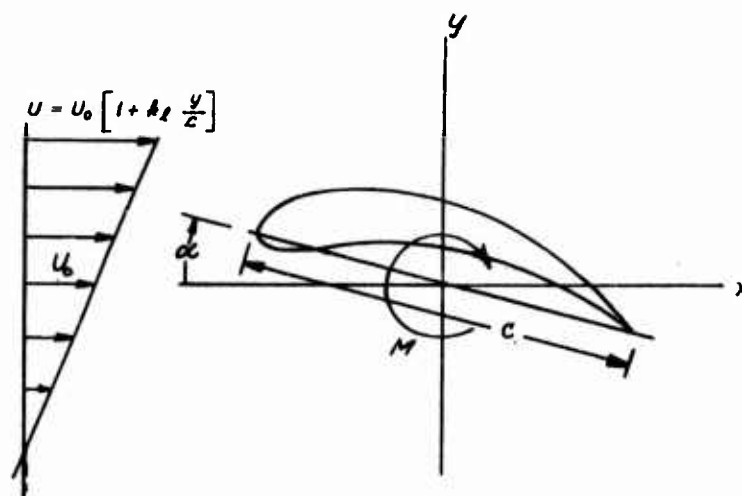


Figure 1 THEORETICAL MODEL OF UNIFORM SHEAR

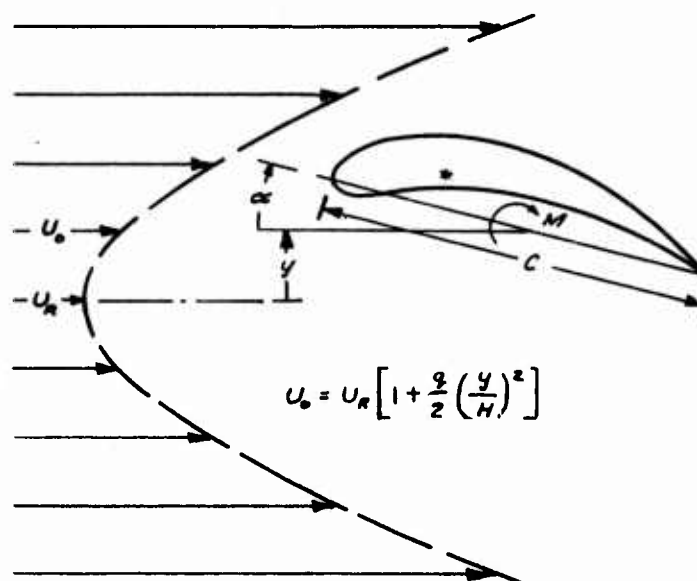


Figure 2 THEORETICAL MODEL OF NON-UNIFORM SHEAR

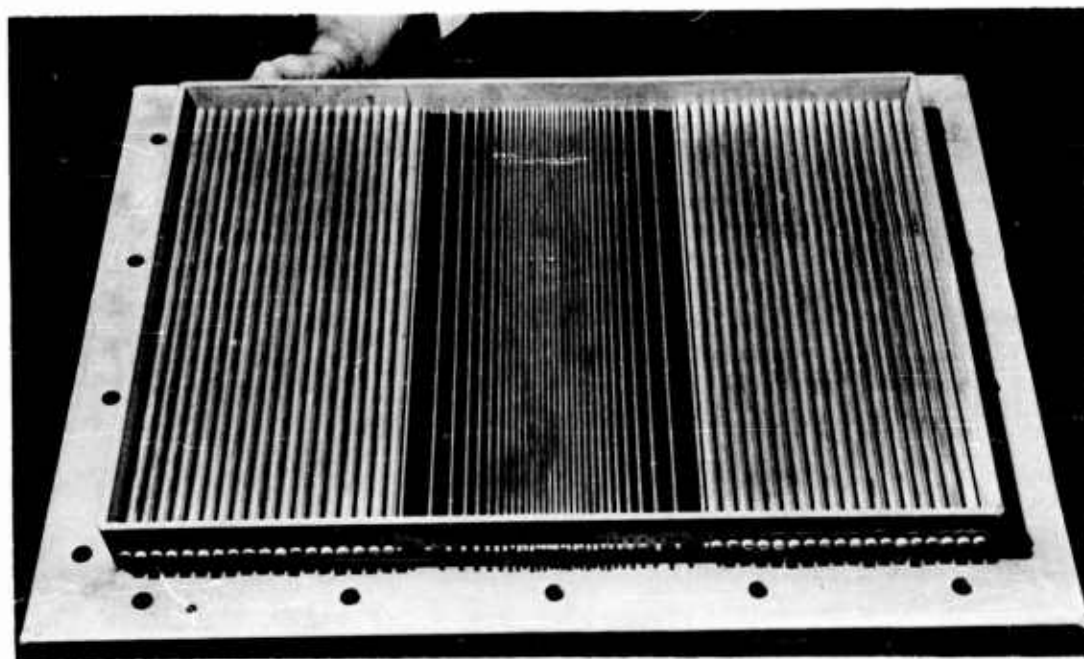
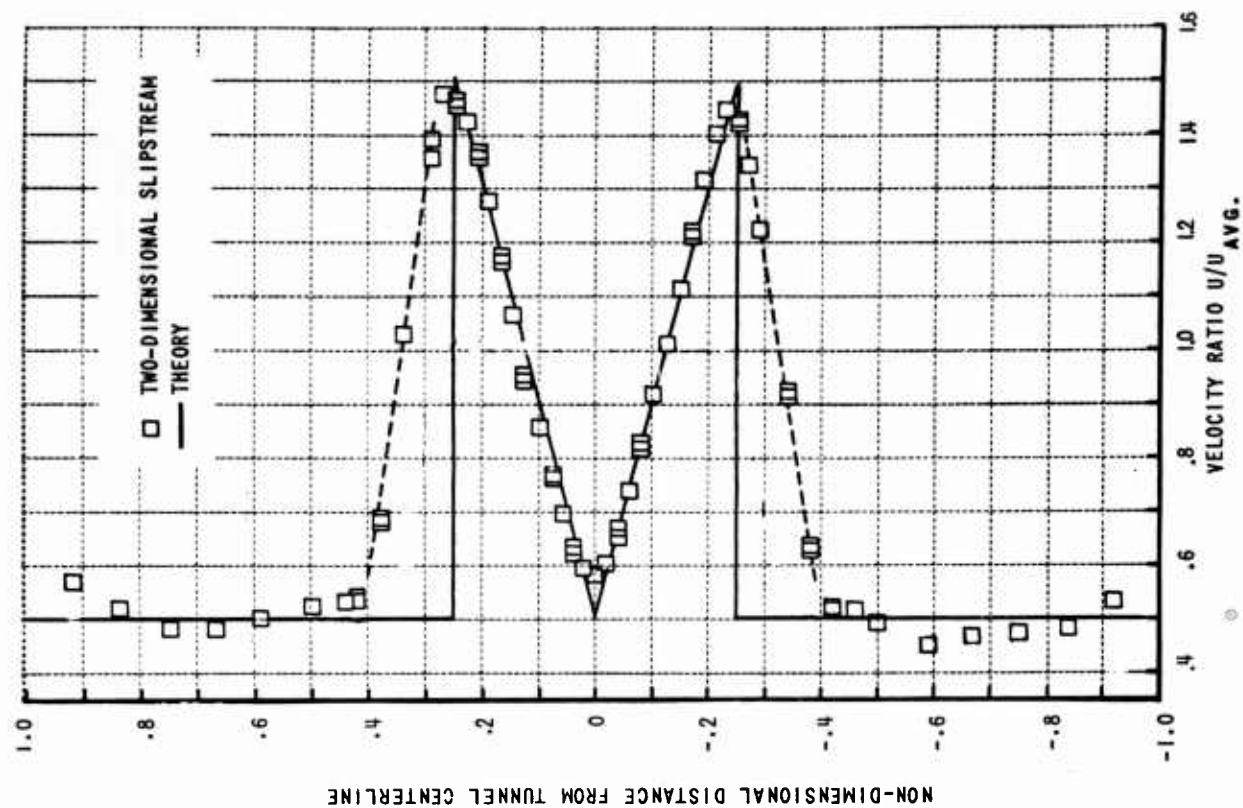


Figure 3 SCREEN FOR TWO-DIMENSIONAL PROPELLER SLIPSTREAM WITH LARGE SHEAR AND FLOW CALIBRATION

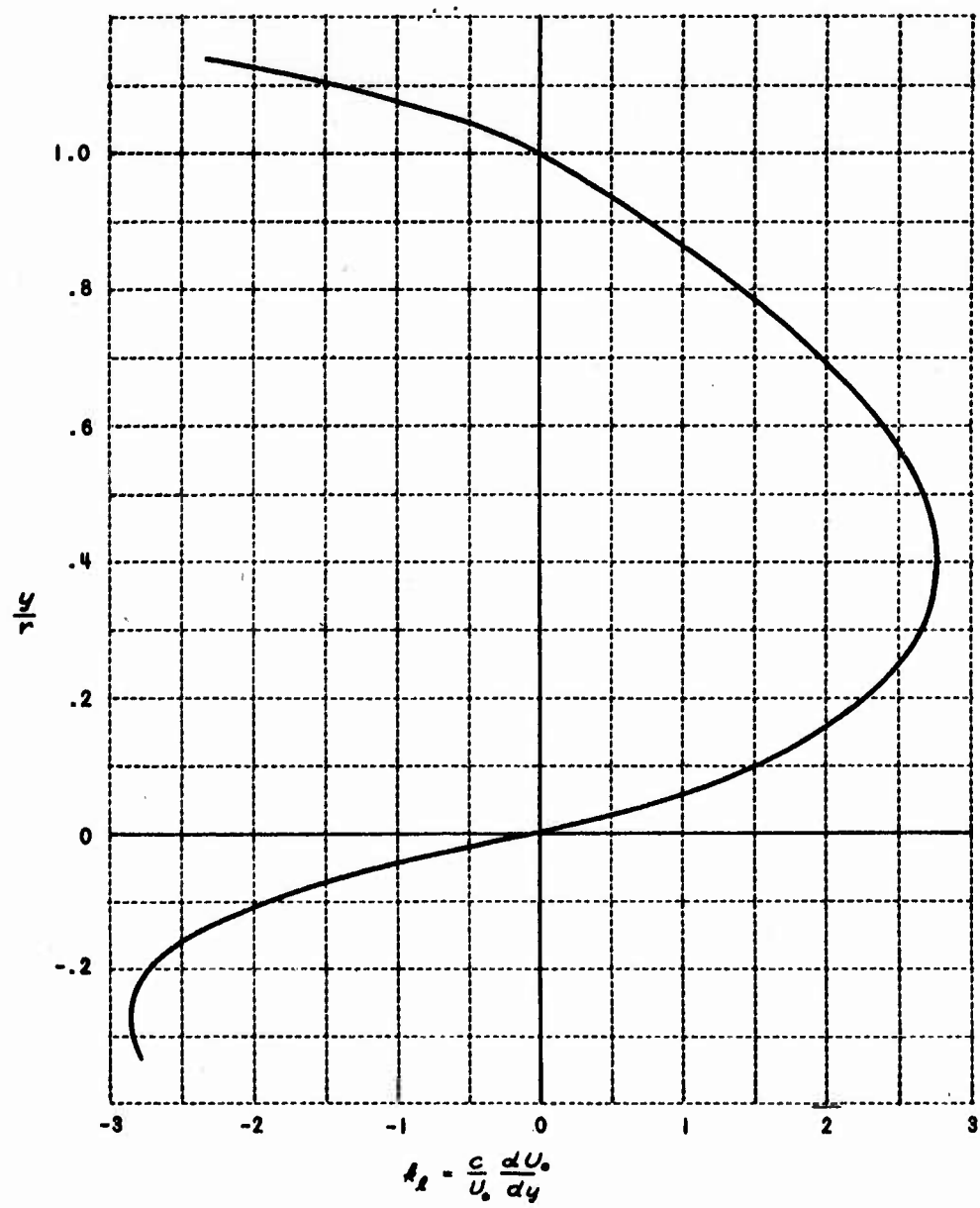


Figure 4 EXPERIMENTAL DISTRIBUTION OF STREAM SHEAR

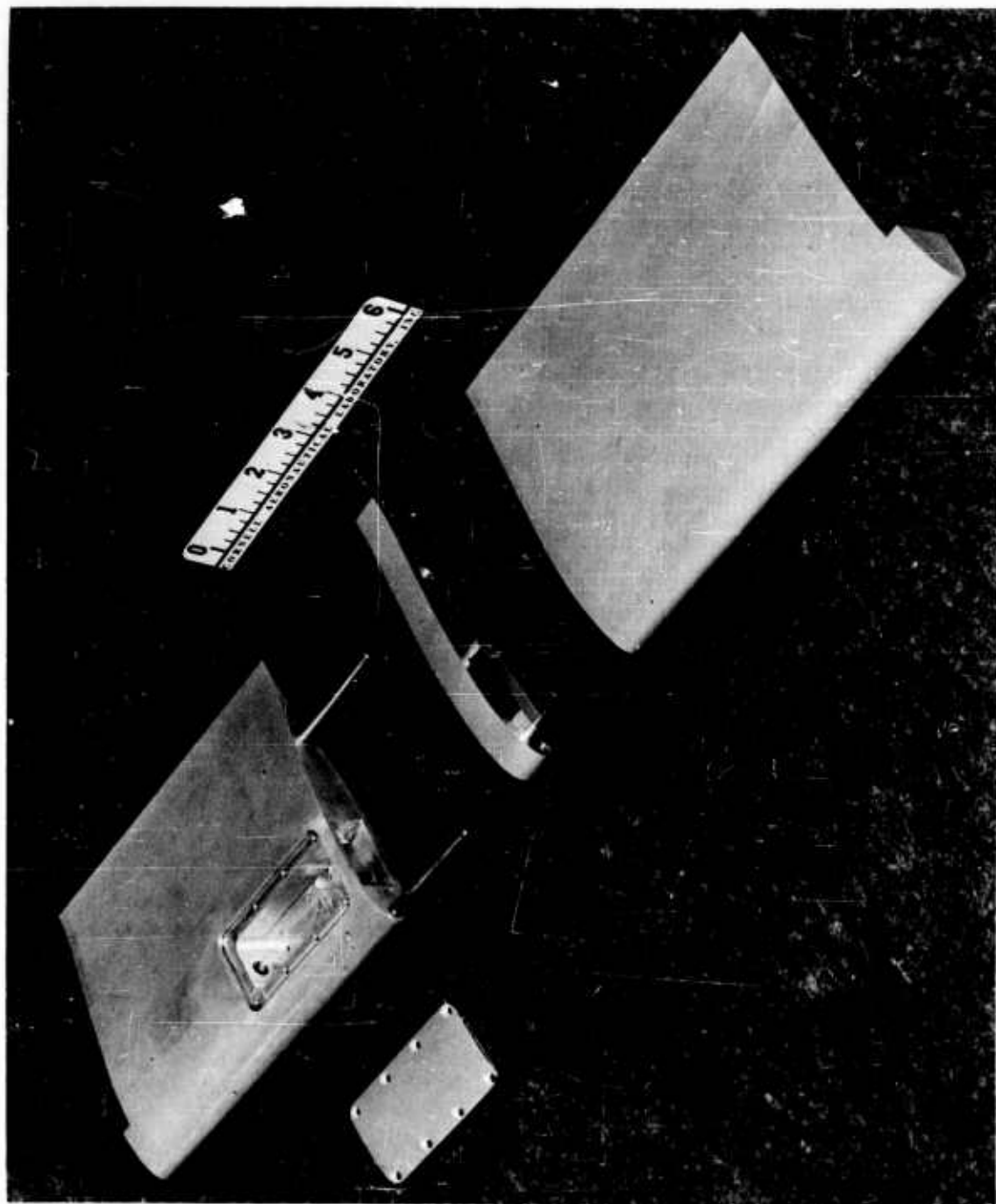


Figure 5 TWO-DIMENSIONAL AIRFOIL MODEL AND FORCE BALANCE

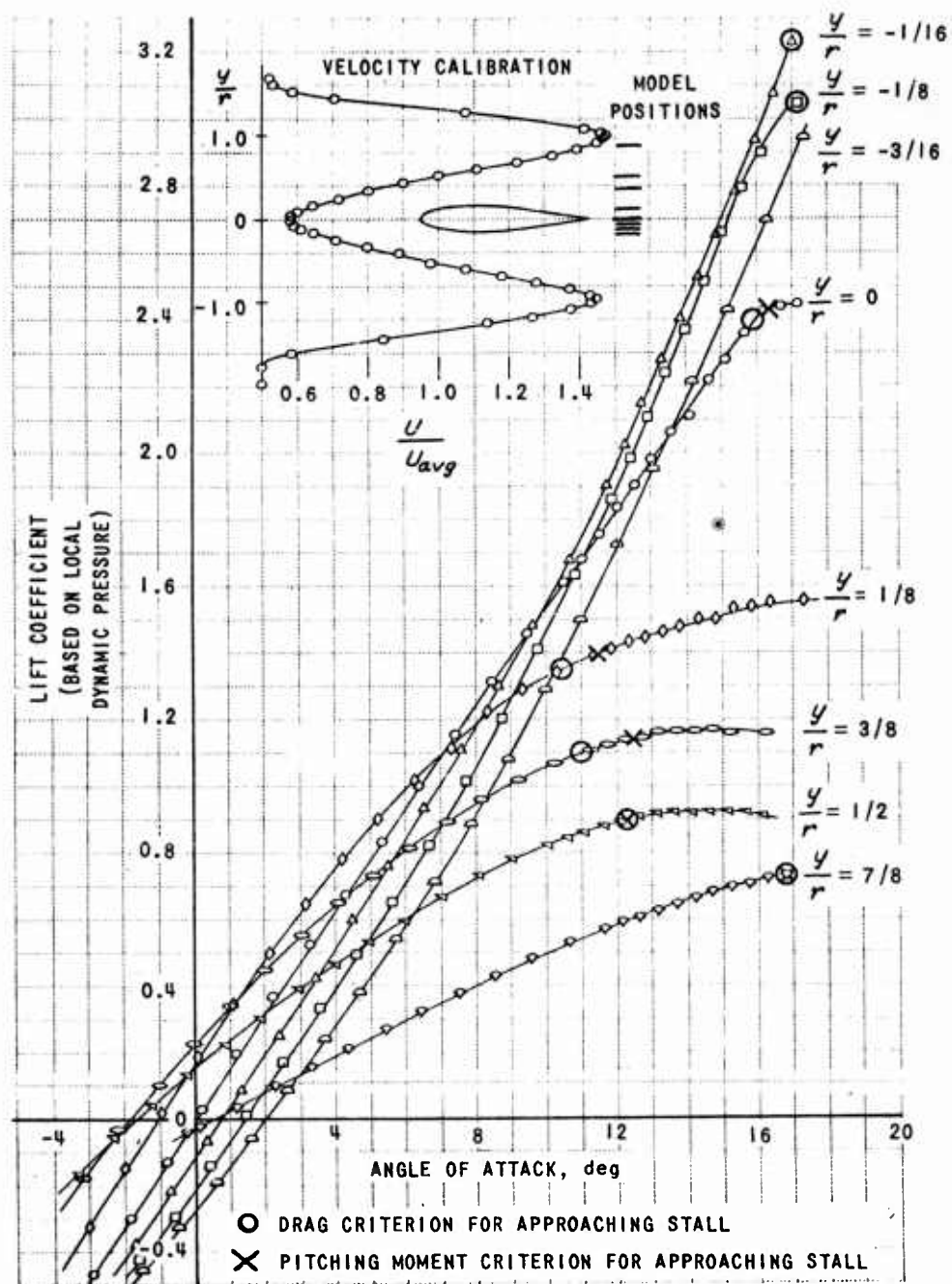


Figure 6 WING SECTION LIFT IN A TWO-DIMENSIONAL PROPELLER SLIPSTREAM

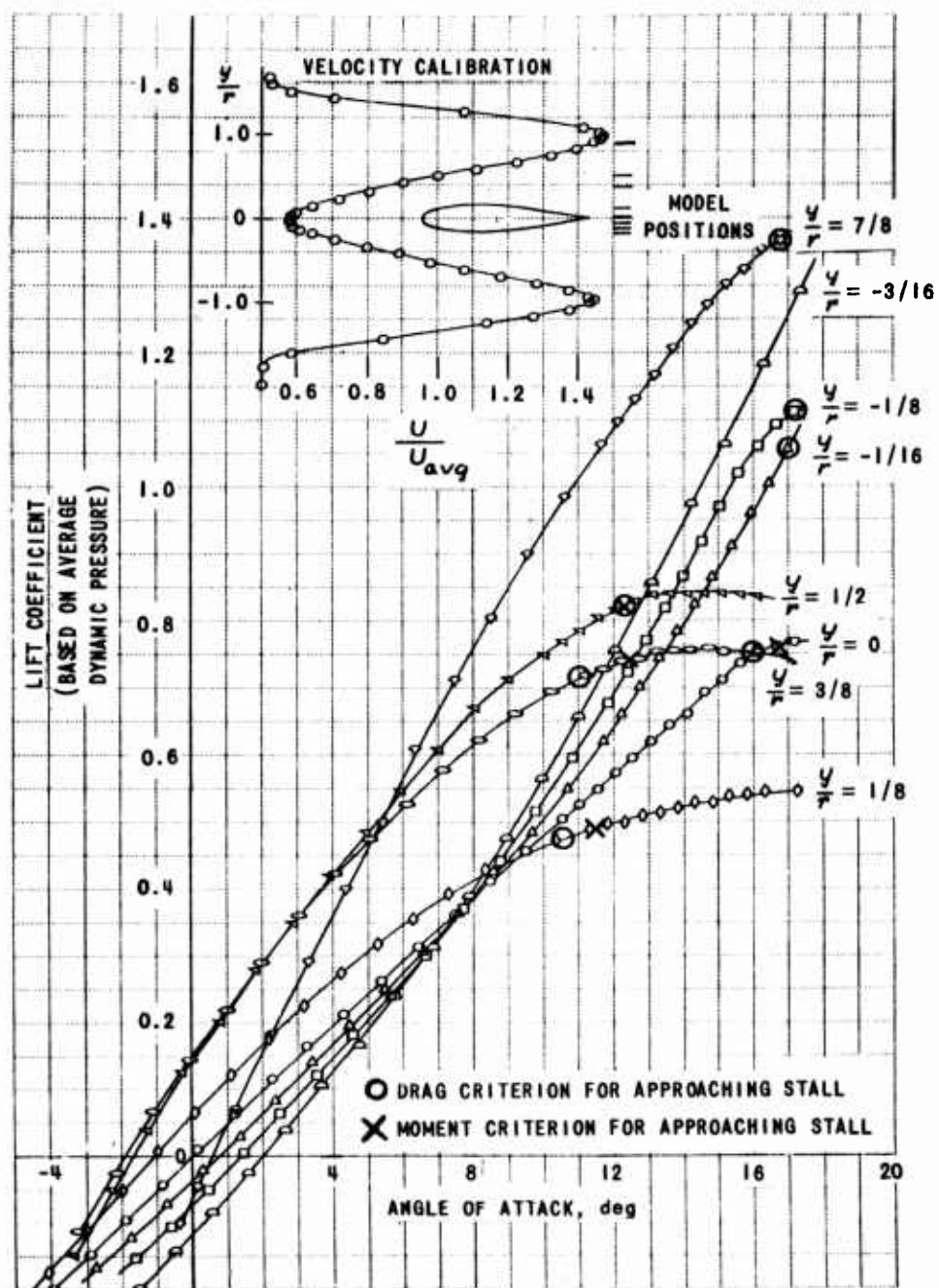


Figure 7 WING SECTION LIFT IN A TWO-DIMENSIONAL PROPELLER SLIPSTREAM

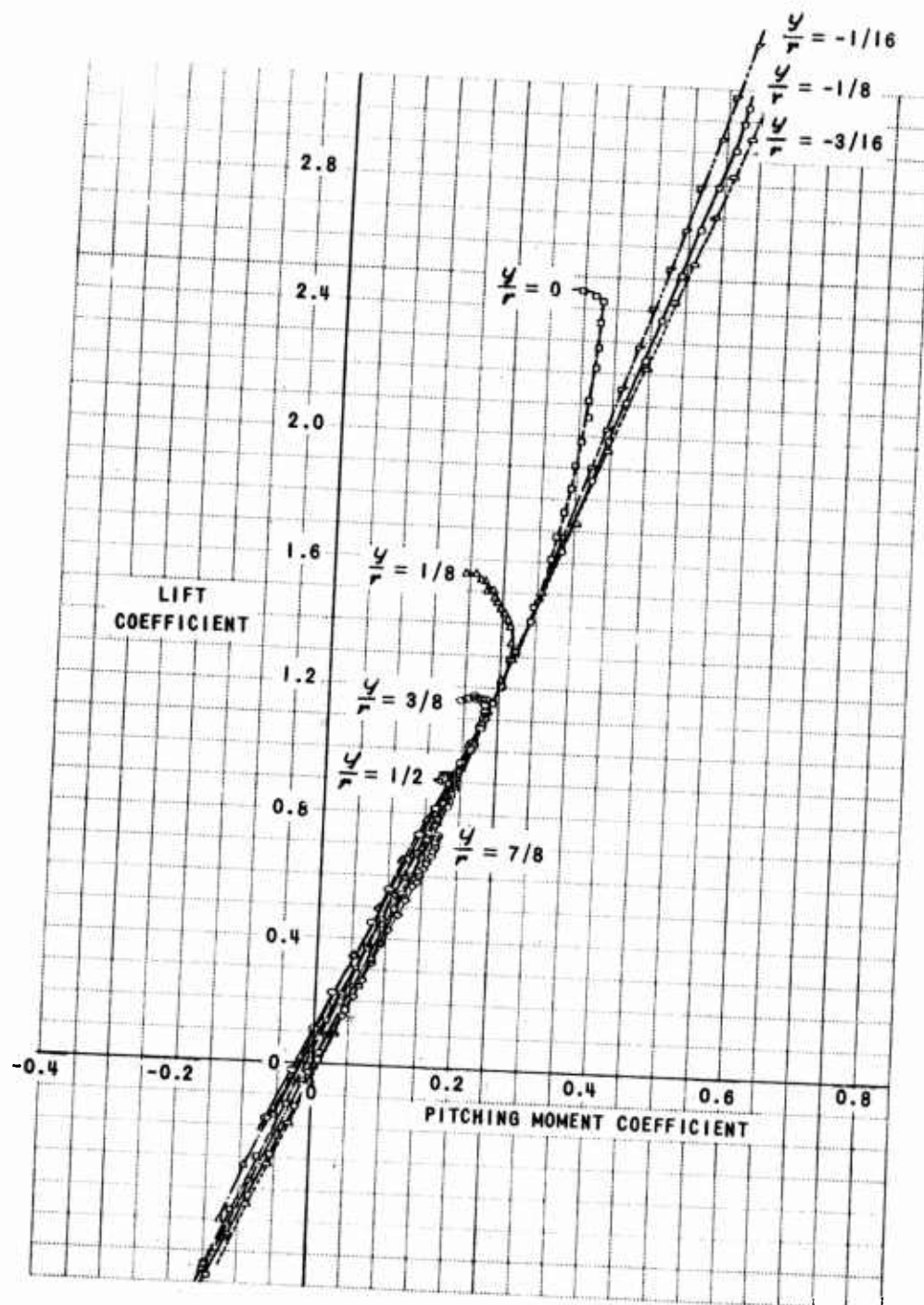


Figure 8 WING SECTION PITCHING MOMENT IN A TWO-DIMENSIONAL PROPELLER SLIPSTREAM

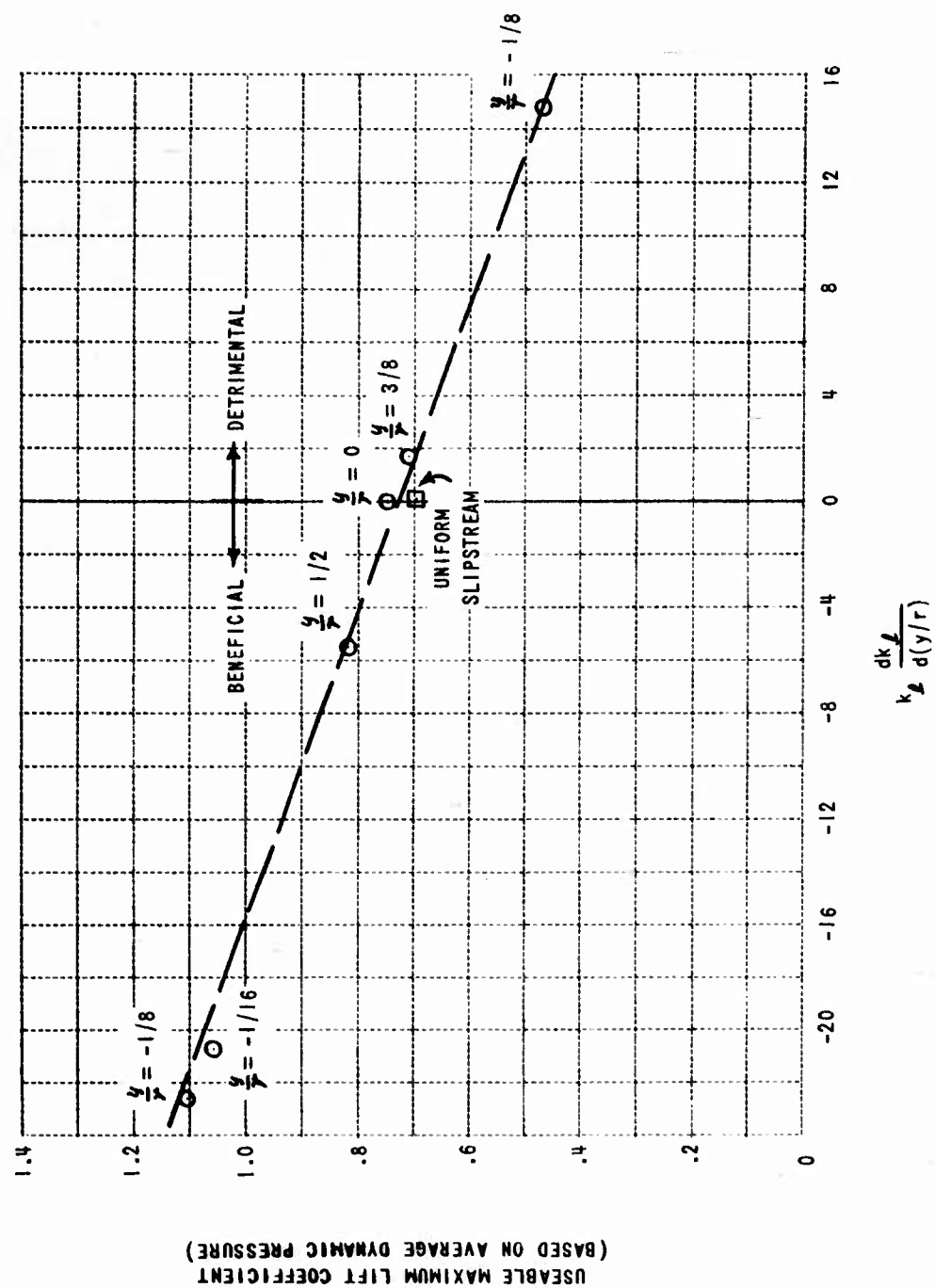


Figure 9 CORRELATION OF MAXIMUM LIFT WITH STEAM PROPERTIES

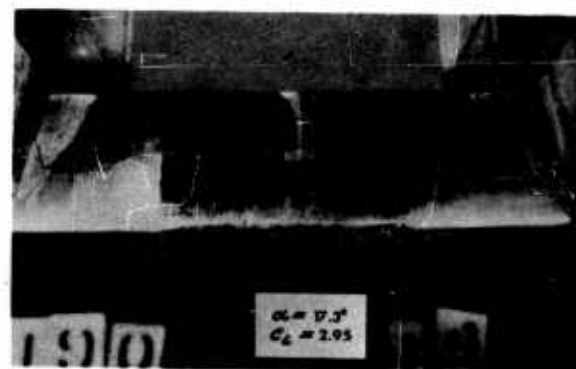


Figure 10 OIL FILM STUDIES OF BOUNDARY LAYER SEPARATION

$y/r = - 3/16$

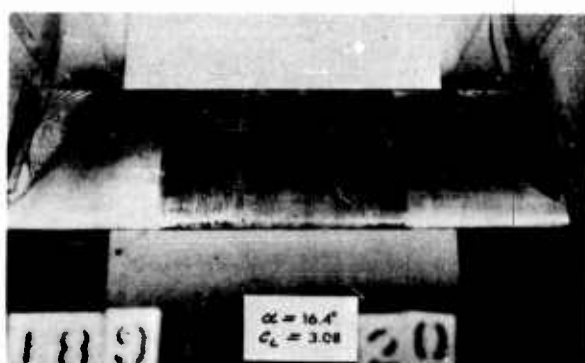
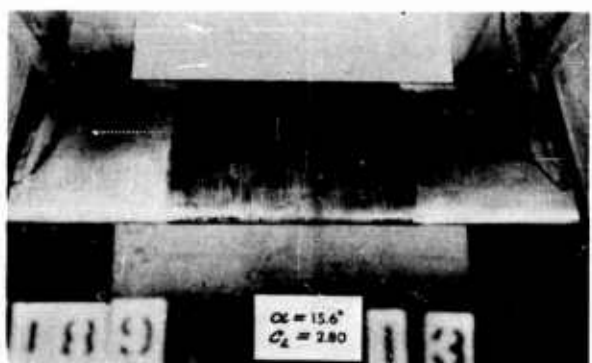
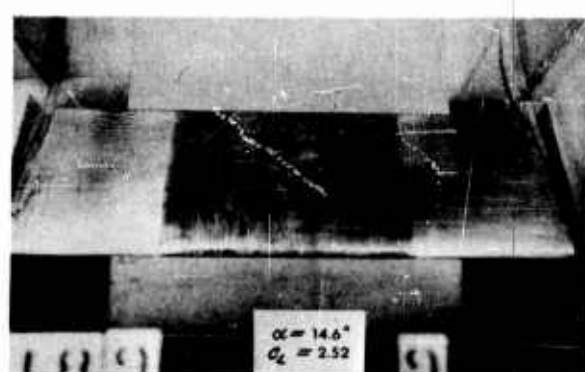
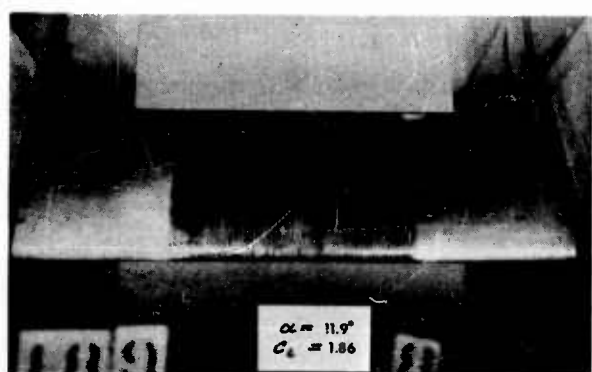
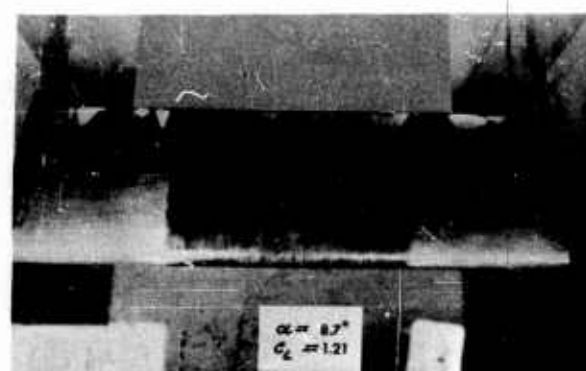
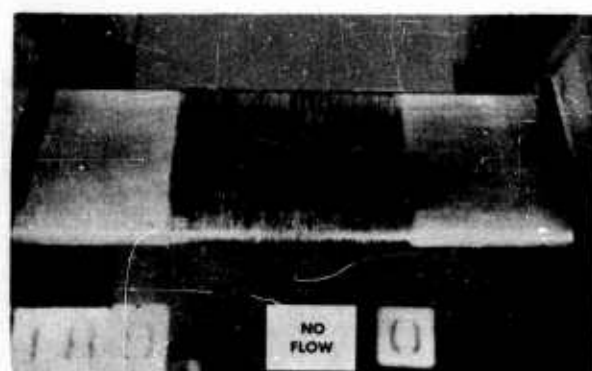


Figure II OIL FILM STUDIES OF BOUNDARY LAYER SEPARATION
 $y/r = -1/8$

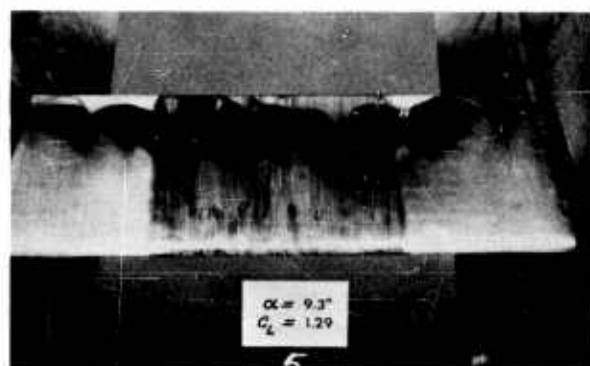
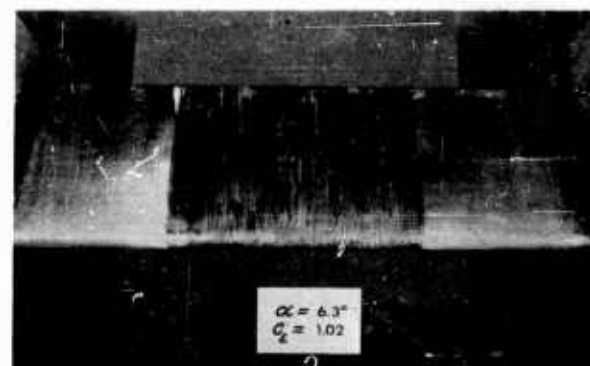
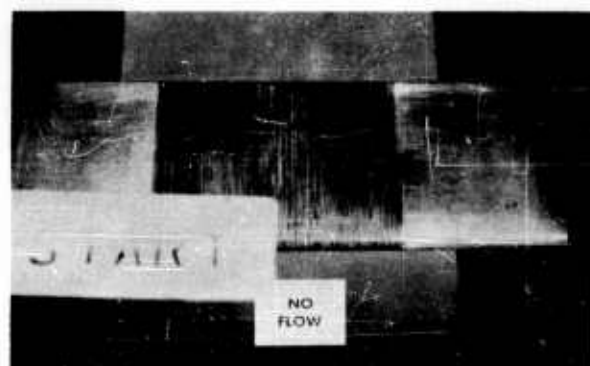


Figure 12 OIL FILM STUDIES OF BOUNDARY LAYER SEPARATION

$$y/\mu = +1/8$$

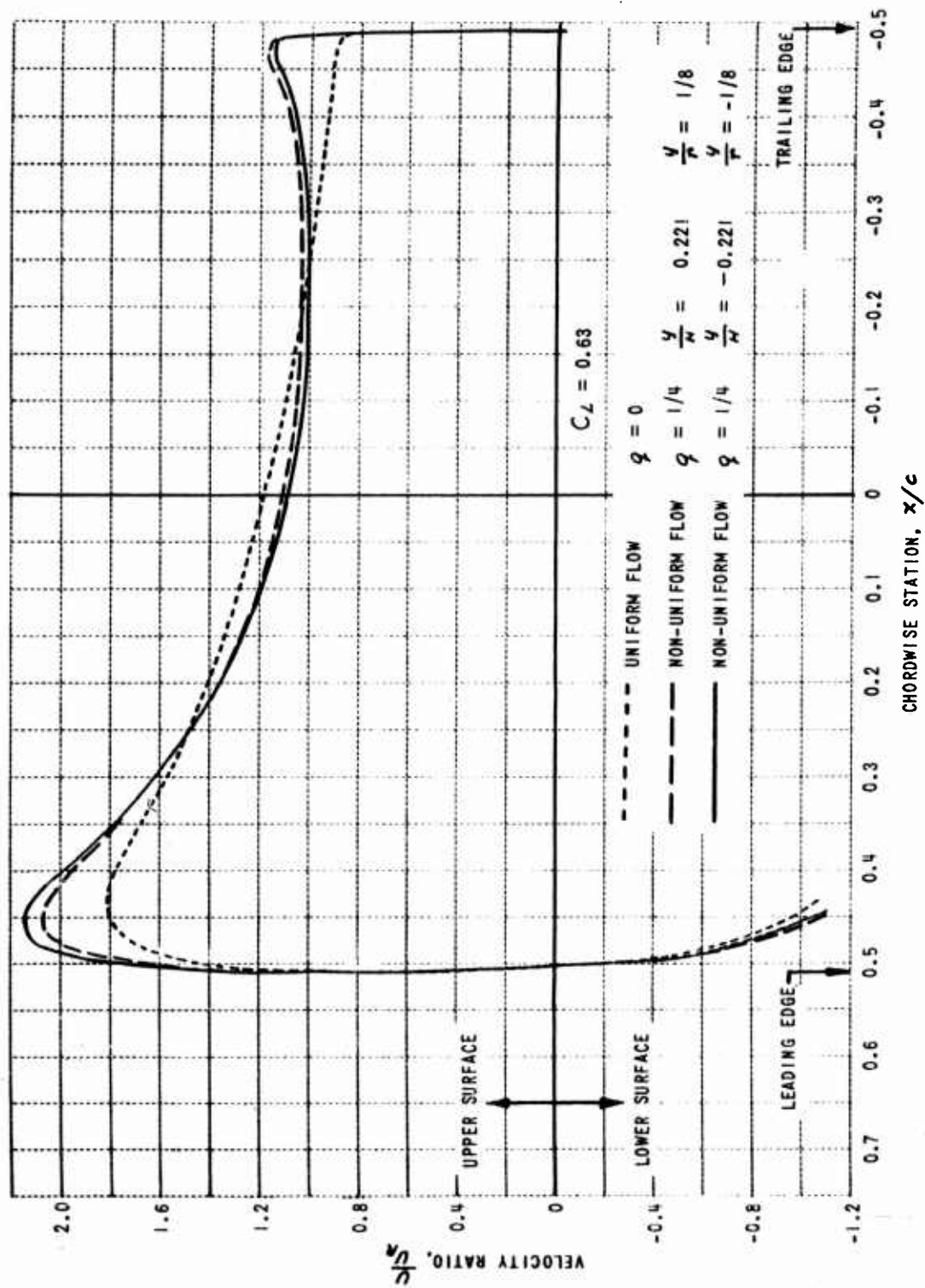


Figure 13 AIRFOIL VELOCITY DISTRIBUTION IN UNIFORM AND NON-UNIFORM FLOW

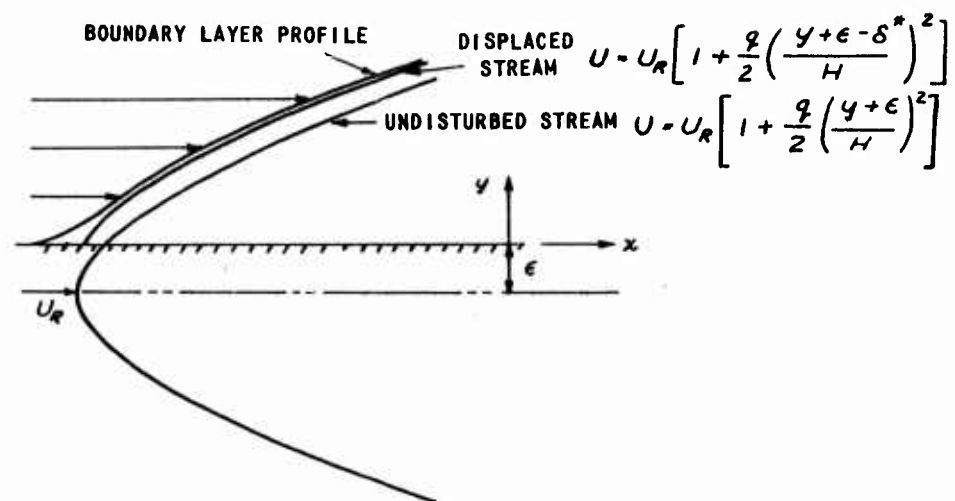


Figure 14 BOUNDARY LAYER COORDINATE SYSTEM

DISTRIBUTION LIST

Chief of Transportation	(2)
ATTN: TCDRC	
ATTN: TCAFO-R	(1)
Department of the Army	
Washington 25, D. C.	
Commanding Officer	
U. S. Army Transportation Research Command	
ATTN: Research Reference Center	(9)
ATTN: Executive for Programs	(1)
ATTN: Aviation Directorate	(3)
ATTN: Military Liaison and Advisory Office	(4)
Fort Eustis, Virginia	
Commanding General	
U. S. Army Transportation Material Command	
ATTN: TCMAD-APU	(1)
P. O. Box 209, Main Office	
St. Louis 66, Missouri	
Commander	
Air Research and Development Command	
ATTN: RDR-LA	(1)
Andrews Air Force Base	
Washington 25, D. C.	
Office of Chief of Research and Development	
ATTN: Air Mobility Division	(1)
Department of the Army	
Washington 25, D. C.	
Commander	
Aeronautical Systems Division	
ATTN: EWAPEL-(Z)	(1)
Air Force Systems Command	
Wright-Patterson Air Force Base, Ohio	
Chief of Naval Research	
Code 461, Maj. L. C. Robertson	(1)
Washington 25, D. C.	
National Aeronautics and Space Administration	
ATTN: Assistant Director for Technical Information	(4)
1520 H Street, Northwest	
Washington 25, D. C.	

Librarian
Langley Research Center
National Aeronautics and Space Administration
Langley Field, Virginia (1)

Ames Research Center
National Aeronautics and Space Agency
ATTN: Library
Moffett Field, California (1)

National Aeronautics and Space Administration
Lewis Research Center
ATTN: Library
21000 Brookpark Road
Cleveland 35, Ohio (1)

John Glennon, Librarian
Institute of the Aerospace Sciences
2 East 64th Street
New York 21, New York (1)

Commander
Armed Services Technical Information Agency
ATTN: TIPCR
Arlington Hall Station
Arlington 12, Virginia (10)

Canadian Army Liaison Officer
Liaison Group, Room 208
U.S. Army Transportation School
Fort Eustis, Virginia (3)

British Joint Services Mission (Army Staff)
ATTN: Lt. Col. R. J. Wade, RE
DAQMG (Mov & Tn)
3100 Massachusetts Avenue, N. W.
Washington 8, D. C. (3)

Office of the Senior Standardization Representative
U.S. Army Standardization Group, Canada
c/o Director of Equipment Policy
Canadian Army Headquarters
Ottawa, Canada (1)

U. S. Army Standardization Group, U. K.
Box 65, U. S. Navy 100
EPO New York, New York (1)

Chief U. S. Army R&D Liaison Group (9851DU) ATTN: USATRECOM LO APO 757 New York, New York	(1)
Bell Aerosystems Company Division of Bell Aerospace Corporation ATTN: Library Buffalo 5, New York	(1)
Bell Helicopter Company Division of Bell Aerospace Corporation ATTN: Library P.O. Box 482 Fort Worth 1, Texas	(1)
Cornell University Engineering Library ATTN: Library Ithaca, New York	(1)
Fairchild Aircraft Division Fairchild Engine and Aircraft Company ATTN: Mr. H. B. Heimbold Hagerstown, Maryland	(1)
Goodyear Aircraft Corporation ATTN: Library Akron, Ohio	(1)
Grumman Aircraft Engineering Corporation ATTN: Library Bethpage, Long Island, New York	(1)
Hiller Aircraft Corporation ATTN: Library Palo Alto, California	(1)
Kaman Aircraft Corporation ATTN: Library Bloomfield, Connecticut	(1)
Lockheed Aircraft Corporation ATTN: Library Marietta, Georgia	(1)
Lockheed Aircraft Corporation ATTN: Library Burbank, California	(1)

McDonnell Aircraft Corporation ATTN: Library St. Louis, Missouri	(1)
Piasecki Aircraft Corporation ATTN: Library Philadelphia 42, Pennsylvania	(1)
Republic Aviation Corporation ATTN: Dr. Theodore Theodorsen Farmingdale, Long Island, New York	(1)
Ryan Aeronautical Company ATTN: Library San Diego, California	(1)
General Dynamics Corporation Convair Division ATTN: Mr. W. A. Martin San Diego, California	(1)
United Aircraft Corporation Sikorsky Aircraft Division ATTN: Library Bridgeport, Connecticut	(1)
Vertol Aircraft Corporation ATTN: Library Morton, Pennsylvania	(1)
RCA Service Company ATTN: Mr. S. Hu 4374 East Speedway Tucson, Arizona	(1)
Massachusetts Institute of Technology ATTN: Mr. Rene Miller Aeronautical Engineering Department Cambridge, Massachusetts	(1)
Mississippi State College State College, Mississippi	(1)
Texas A & M College ATTN: Mr. A. Gail College Station, Texas	(1)

<p>AD-</p> <p>Cornell Aeronautical Laboratory, Inc., Buffalo, New York</p> <p>THE INFLUENCE OF TWO-DIMENSIONAL STREAM SHEAR ON AIRFOIL MAXIMUM LIFT - R. J. Vidal, J. T. Curtis, and J. H. Hilton.</p> <p>CAL Report No. AL-1190-A-7, August 1961, 55 pp. - illus. (Contract DA 44-177-TC-439) Proj. 9R38-01-000, Task 902</p> <p>The effects of stream velocity gradients on airfoil maximum lift are defined with experimental data obtained in a simulated two-dimensional slipstream. The experimental results show that when positioned near the slipstream plane of symmetry, the airfoil maximum lift varies markedly with location in the slipstream. In moving the airfoil from above to below the slipstream plane of symmetry through a total distance corresponding to the airfoil thickness, force data and boundary-layer observations show that boundary-layer separation is delayed to higher angles of attack, and the airfoil maximum lift is doubled.</p> <p>over</p>	<p>UNCLASSIFIED</p> <ol style="list-style-type: none"> 1. STOL/VTOL 2. Contract DA 44-177-TC-439 <p>UNCLASSIFIED</p>
--	--

<p>AD-</p> <p>Cornell Aeronautical Laboratory, Inc., Buffalo, New York</p> <p>THE INFLUENCE OF TWO-DIMENSIONAL STREAM SHEAR ON AIRFOIL MAXIMUM LIFT - R. J. Vidal, J. T. Curtis, and J. H. Hilton.</p> <p>CAL Report No. AL-1190-A-7, August 1961, 55 pp. - illus. (Contract DA 44-177-TC-439) Proj. 9R38-01-000, Task 902</p> <p>The effects of stream velocity gradients on airfoil maximum lift are defined with experimental data obtained in a simulated two-dimensional slipstream. The experimental results show that when positioned near the slipstream plane of symmetry, the airfoil maximum lift varies markedly with location in the slipstream. In moving the airfoil from above to below the slipstream plane of symmetry through a total distance corresponding to the airfoil thickness, force data and boundary-layer observations show that boundary-layer separation is delayed to higher angles of attack, and the airfoil maximum lift is doubled.</p> <p>over</p>	<p>UNCLASSIFIED</p> <ol style="list-style-type: none"> 1. STOL/VTOL 2. Contract DA 44-177-TC-439 <p>UNCLASSIFIED</p>
--	--

<p>AD-</p> <p>Cornell Aeronautical Laboratory, Inc., Buffalo, New York</p> <p>THE INFLUENCE OF TWO-DIMENSIONAL STREAM SHEAR ON AIRFOIL MAXIMUM LIFT - R. J. Vidal, J. T. Curtis, and J. H. Hilton.</p> <p>CAL Report No. AL-1190-A-7, August 1961, 55 pp. - illus. (Contract DA 44-177-TC-439) Proj. 9R38-01-000, Task 902</p> <p>The effects of stream velocity gradients on airfoil maximum lift are defined with experimental data obtained in a simulated two-dimensional slipstream. The experimental results show that when positioned near the slipstream plane of symmetry, the airfoil maximum lift varies markedly with location in the slipstream. In moving the airfoil from above to below the slipstream plane of symmetry through a total distance corresponding to the airfoil thickness, force data and boundary-layer observations show that boundary-layer separation is delayed to higher angles of attack, and the airfoil maximum lift is doubled.</p> <p>over</p>	<p>UNCLASSIFIED</p> <ol style="list-style-type: none"> 1. STOL/VTOL 2. Contract DA 44-177-TC-439 <p>UNCLASSIFIED</p>
--	--

<p>AD-</p> <p>Cornell Aeronautical Laboratory, Inc., Buffalo, New York</p> <p>THE INFLUENCE OF TWO-DIMENSIONAL STREAM SHEAR ON AIRFOIL MAXIMUM LIFT - R. J. Vidal, J. T. Curtis, and J. H. Hilton.</p> <p>CAL Report No. AL-1190-A-7, August 1961, 55 pp. - illus. (Contract DA 44-177-TC-439) Proj. 9R38-01-000, Task 902</p> <p>The effects of stream velocity gradients on airfoil maximum lift are defined with experimental data obtained in a simulated two-dimensional slipstream. The experimental results show that when positioned near the slipstream plane of symmetry, the airfoil maximum lift varies markedly with location in the slipstream. In moving the airfoil from above to below the slipstream plane of symmetry through a total distance corresponding to the airfoil thickness, force data and boundary-layer observations show that boundary-layer separation is delayed to higher angles of attack, and the airfoil maximum lift is doubled.</p> <p>over</p>	<p>UNCLASSIFIED</p> <ol style="list-style-type: none"> 1. STOL/VTOL 2. Contract DA 44-177-TC-439 <p>UNCLASSIFIED</p>
--	--

UNCLASSIFIED

It is concluded that the destalling effect observed in the nonuniform slipstream is not associated with slipstream boundary interference, but stems from the influence of the large local slipstream shear on airfoil characteristics. The effects of uniform and nonuniform shear on airfoil lift and pressure distribution are discussed, within the framework of existing first-order, small-shear theory, to show that these effects of shear tend to promote stall. A Pohlhausen calculation of the laminar boundary layer in a stream with shear is used to identify and to assess the effects of stream shear on boundary-layer separation criteria. It is demonstrated that these effects are negligibly small, and that the uniform flow criterion applies. It is concluded on the basis of the experimental data that the observed destalling phenomenon stems from a shear effect of higher order than those treated in the inviscid theories. It is hypothesized that it is a second-order effect, fixed by the product of the stream shear and the derivative of the shear, which was large in the present experiments.

UNCLASSIFIED

UNCLASSIFIED

It is concluded that the destalling effect observed in the nonuniform slipstream is not associated with slipstream boundary interference, but stems from the influence of the large local slipstream shear on airfoil characteristics. The effects of uniform and nonuniform shear on airfoil lift and pressure distribution are discussed, within the framework of existing first-order, small-shear theory, to show that these effects of shear tend to promote stall. A Pohlhausen calculation of the laminar boundary layer in a stream with shear is used to identify and to assess the effects of stream shear on boundary-layer separation criteria. It is demonstrated that these effects are negligibly small, and that the uniform flow criterion applies. It is concluded on the basis of the experimental data that the observed destalling phenomenon stems from a shear effect of higher order than those treated in the inviscid theories. It is hypothesized that it is a second-order effect, fixed by the product of the stream shear and the derivative of the shear, which was large in the present experiments.

UNCLASSIFIED

UNCLASSIFIED

It is concluded that the destalling effect observed in the nonuniform slipstream is not associated with slipstream boundary interference, but stems from the influence of the large local slipstream shear on airfoil characteristics. The effects of uniform and nonuniform shear on airfoil lift and pressure distribution are discussed, within the framework of existing first-order, small-shear theory, to show that these effects of shear tend to promote stall. A Pohlhausen calculation of the laminar boundary layer in a stream with shear is used to identify and to assess the effects of stream shear on boundary-layer separation criteria. It is demonstrated that these effects are negligibly small, and that the uniform flow criterion applies. It is concluded on the basis of the experimental data that the observed destalling phenomenon stems from a shear effect of higher order than those treated in the inviscid theories. It is hypothesized that it is a second-order effect, fixed by the product of the stream shear and the derivative of the shear, which was large in the present experiments.

UNCLASSIFIED

UNCLASSIFIED

It is concluded that the destalling effect observed in the nonuniform slipstream is not associated with slipstream boundary interference, but stems from the influence of the large local slipstream shear on airfoil characteristics. The effects of uniform and nonuniform shear on airfoil lift and pressure distribution are discussed, within the framework of existing first-order, small-shear theory, to show that these effects of shear tend to promote stall. A Pohlhausen calculation of the laminar boundary layer in a stream with shear is used to identify and to assess the effects of stream shear on boundary-layer separation criteria. It is demonstrated that these effects are negligibly small, and that the uniform flow criterion applies. It is concluded on the basis of the experimental data that the observed destalling phenomenon stems from a shear effect of higher order than those treated in the inviscid theories. It is hypothesized that it is a second-order effect, fixed by the product of the stream shear and the derivative of the shear, which was large in the present experiments.

UNCLASSIFIED

<p>AD-</p> <p>Cornell Aeronautical Laboratory, Inc., Buffalo, New York</p> <p>THE INFLUENCE OF TWO-DIMENSIONAL STREAM SHEAR ON AIRFOIL MAXIMUM LIFT - R. J. Vidal, J. T. Curtis, and J. H. Hilton.</p> <p>CAL Report No. AL-1190-A-7, August 1961, 55 pp. - illus. (Contract DA 44-177-TC-439) Proj. 9R38-01-000, Task 902</p> <p>The effects of stream velocity gradients on airfoil maximum lift are defined with experimental data obtained in a simulated two-dimensional slipstream. The experimental results show that when maximum lift varies markedly with location in the slipstream. In moving the airfoil from above to below the slipstream plane of symmetry through a total distance corresponding to the airfoil thickness, force data and boundary-layer observations show that boundary-layer separation is delayed to higher angles of attack, and the airfoil maximum lift is doubled.</p>	<p>UNCLASSIFIED</p> <p>1. STOL/VTOL</p> <p>2. Contract DA 44-177-TC-439</p> <p>UNCLASSIFIED</p>
--	---

over

<p>AD-</p> <p>Cornell Aeronautical Laboratory, Inc., Buffalo, New York</p> <p>THE INFLUENCE OF TWO-DIMENSIONAL STREAM SHEAR ON AIRFOIL MAXIMUM LIFT - R. J. Vidal, J. T. Curtis, and J. H. Hilton.</p> <p>CAL Report No. AL-1190-A-7, August 1961, 55 pp. - illus. (Contract DA 44-177-TC-439) Proj. 9R38-01-000, Task 902</p> <p>The effects of stream velocity gradients on airfoil maximum lift are defined with experimental data obtained in a simulated two-dimensional slipstream. The experimental results show that when maximum lift varies markedly with location in the slipstream. In moving the airfoil from above to below the slipstream plane of symmetry through a total distance corresponding to the airfoil thickness, force data and boundary-layer observations show that boundary-layer separation is delayed to higher angles of attack, and the airfoil maximum lift is doubled.</p>	<p>UNCLASSIFIED</p> <p>1. STOL/VTOL</p> <p>2. Contract DA 44-177-TC-439</p> <p>UNCLASSIFIED</p>
--	---

over

<p>AD-</p> <p>Cornell Aeronautical Laboratory, Inc., Buffalo, New York</p> <p>THE INFLUENCE OF TWO-DIMENSIONAL STREAM SHEAR ON AIRFOIL MAXIMUM LIFT - R. J. Vidal, J. T. Curtis, and J. H. Hilton.</p> <p>CAL Report No. AL-1190-A-7, August 1961, 55 pp. - illus. (Contract DA 44-177-TC-439) Proj. 9R38-01-000, Task 902</p> <p>The effects of stream velocity gradients on airfoil maximum lift are defined with experimental data obtained in a simulated two-dimensional slipstream. The experimental results show that when maximum lift varies markedly with location in the slipstream. In moving the airfoil from above to below the slipstream plane of symmetry through a total distance corresponding to the airfoil thickness, force data and boundary-layer observations show that boundary-layer separation is delayed to higher angles of attack, and the airfoil maximum lift is doubled.</p>	<p>UNCLASSIFIED</p> <p>1. STOL/VTOL</p> <p>2. Contract DA 44-177-TC-439</p> <p>UNCLASSIFIED</p>
--	---

over

<p>AD-</p> <p>Cornell Aeronautical Laboratory, Inc., Buffalo, New York</p> <p>THE INFLUENCE OF TWO-DIMENSIONAL STREAM SHEAR ON AIRFOIL MAXIMUM LIFT - R. J. Vidal, J. T. Curtis, and J. H. Hilton.</p> <p>CAL Report No. AL-1190-A-7, August 1961, 55 pp. - illus. (Contract DA 44-177-TC-439) Proj. 9R38-01-000, Task 902</p> <p>The effects of stream velocity gradients on airfoil maximum lift are defined with experimental data obtained in a simulated two-dimensional slipstream. The experimental results show that when maximum lift varies markedly with location in the slipstream. In moving the airfoil from above to below the slipstream plane of symmetry through a total distance corresponding to the airfoil thickness, force data and boundary-layer observations show that boundary-layer separation is delayed to higher angles of attack, and the airfoil maximum lift is doubled.</p>	<p>UNCLASSIFIED</p> <p>1. STOL/VTOL</p> <p>2. Contract DA 44-177-TC-439</p> <p>UNCLASSIFIED</p>
--	---

over

UNCLASSIFIED	<p>It is concluded that the destalling effect observed in the nonuniform slipstream is not associated with slipstream boundary interference, but stems from the influence of the large local slipstream shear on airfoil characteristics. The effects of uniform and nonuniform shear on airfoil lift and pressure distribution are discussed, within the framework of existing first-order, small-shear theory, to show that these effects of shear tend to promote stall. A Pohlhausen calculation of the laminar boundary layer in a stream with shear is used to identify and to assess the effects of stream shear on boundary-layer separation criteria. It is demonstrated that these effects are negligibly small, and that the uniform flow criterion applies. It is concluded on the basis of the experimental data that the observed destalling phenomenon stems from a shear effect of higher order than those treated in the inviscid theories. It is hypothesized that it is a second-order effect, fixed by the product of the stream shear and the derivative of the shear, which was large in the present experiments.</p>
UNCLASSIFIED	UNCLASSIFIED

UNCLASSIFIED	<p>It is concluded that the destalling effect observed in the nonuniform slipstream is not associated with slipstream boundary interference, but stems from the influence of the large local slipstream shear on airfoil characteristics. The effects of uniform and nonuniform shear on airfoil lift and pressure distribution are discussed, within the framework of existing first-order, small-shear theory, to show that these effects of shear tend to promote stall. A Pohlhausen calculation of the laminar boundary layer in a stream with shear is used to identify and to assess the effects of stream shear on boundary-layer separation criteria. It is demonstrated that these effects are negligibly small, and that the uniform flow criterion applies. It is concluded on the basis of the experimental data that the observed destalling phenomenon stems from a shear effect of higher order than those treated in the inviscid theories. It is hypothesized that it is a second-order effect, fixed by the product of the stream shear and the derivative of the shear, which was large in the present experiments.</p>
UNCLASSIFIED	UNCLASSIFIED

UNCLASSIFIED	<p>It is concluded that the destalling effect observed in the nonuniform slipstream is not associated with slipstream boundary interference, but stems from the influence of the large local slipstream shear on airfoil characteristics. The effects of uniform and nonuniform shear on airfoil lift and pressure distribution are discussed, within the framework of existing first-order, small-shear theory, to show that these effects of shear tend to promote stall. A Pohlhausen calculation of the laminar boundary layer in a stream with shear is used to identify and to assess the effects of stream shear on boundary-layer separation criteria. It is demonstrated that these effects are negligibly small, and that the uniform flow criterion applies. It is concluded on the basis of the experimental data that the observed destalling phenomenon stems from a shear effect of higher order than those treated in the inviscid theories. It is hypothesized that it is a second-order effect, fixed by the product of the stream shear and the derivative of the shear, which was large in the present experiments.</p>
UNCLASSIFIED	UNCLASSIFIED

UNCLASSIFIED	<p>It is concluded that the destalling effect observed in the nonuniform slipstream is not associated with slipstream boundary interference, but stems from the influence of the large local slipstream shear on airfoil characteristics. The effects of uniform and nonuniform shear on airfoil lift and pressure distribution are discussed, within the framework of existing first-order, small-shear theory, to show that these effects of shear tend to promote stall. A Pohlhausen calculation of the laminar boundary layer in a stream with shear is used to identify and to assess the effects of stream shear on boundary-layer separation criteria. It is demonstrated that these effects are negligibly small, and that the uniform flow criterion applies. It is concluded on the basis of the experimental data that the observed destalling phenomenon stems from a shear effect of higher order than those treated in the inviscid theories. It is hypothesized that it is a second-order effect, fixed by the product of the stream shear and the derivative of the shear, which was large in the present experiments.</p>
UNCLASSIFIED	UNCLASSIFIED

UNCLASSIFIED

UNCLASSIFIED